ELSEVIER

Coordination Chemistry Reviews
222 (2001) 57–102

COORDINATION CHEMISTRY REVIEWS

www.elsevier.com/locate/ccr

Calixpyrroles II☆

Philip A. Gale [a,*,1], Pavel Anzenbacher Jr. [b,c,2], Jonathan L. Sessler [b,3,*]

[a] *Department of Chemistry, University of Southampton, Highfield, Southampton SO17 1BJ, UK*
[b] *Department of Chemistry and Biochemistry and Institute for Cellular and Molecular Biology, The University of Texas at Austin, Austin, TX 78712-1167, USA*
[c] *Department of Chemistry and Center for Photochemical Sciences, Bowling Green State University, Bowling Green, OH 43403, USA*

Received 19 October 2000; accepted 27 January 2001

Contents

☆ For Part I see P.A. Gale, J.L. Sessler and V. Král, Chem. Commun. (1998) 1.

* Corresponding authors.
E-mail addresses: philip.gale@soton.ac.uk (P.A. Gale), pavel@bgnet.bgsu.edu (P. Anzenbacher Jr.), sessler@mail.utexas.edu (J.L. Sessler).
[1] Fax: +44-23-80596805
[2] Fax: +1-419-372-9809
[3] Fax: +1-512-471-7550

PII: S0010-8545(01)00346-0

Abstract

This review article is the second in a series covering advances in the synthetic and molecular recognition chemistry of calixpyrrole macrocycles (*meso*-octasubstituted porphyrinogens). Significant progress has been made in the last three years in the use of calix[4]pyrroles as redox-active or optical sensors for anions. This period has also been marked by a number of preparative advances, including the synthesis of *N*-confused calix[4]pyrroles, the synthesis of extended cavity calix[4]pyrroles, and the synthesis of 'higher order' or 'expanded' calix[*n*]pyrroles ($n > 4$).

Keywords: Calixpyrrole; Anion binding; Porphyrinogen; Sensors; Macrocycles

1. Introduction

The calixpyrroles (*meso*-octasubstituted porphyrinogens) are a venerable class of macrocycles, first synthesized by Baeyer in the nineteenth century by condensing pyrrole and acetone in the presence of an acid (to produce *meso*-octamethylcalix[4]pyrrole **1**) [1]. After lying virtually dormant in the literature for nearly a century, interest in these macrocycles was renewed in the 1990s by the extensive work of Floriani and co-workers on the metallation and attendant synthetic chemistry of deprotonated calixpyrroles. Our interest in calixpyrroles stemmed from our discovery in the mid-1990s that the NH array present in these species can act as a binding site for anionic and neutral guest species [2,3]. The formation of an anion-calixpyrrole complex is accompanied by a dramatic change in the conformation of the macrocycle (Scheme 1). Up until this point these macrocycles had been known as porphyrinogens. However, their interesting conformational behavior drew our attention to the clear analogy between them and the calix[4]arenes [4]. This analogy, coupled with the fact that as these species carry eight alkyl or aryl groups in the *meso*-positions and hence are not susceptible to oxidation (to produce either porphyrin or less oxidized macrocyclic products), led us to propose that they should be re-named as calix[4]pyrroles. To our delight, the synthetic and molecular recognition chemistry of the calixpyrroles is now being investigated by a number of research groups worldwide. The purpose of this review is to highlight the advances made in this branch of chemistry over the last three years thereby updating a previously published review [5]. The present review does not cover the metallation chemistry of these macrocycles or any associated synthetic chemistry. Two excellent accounts of this chemistry have recently appeared to which the interested reader is directed [6,7]. Additionally, this review does not cover recent advances in the chemistry of calixpyrrole–porphyrin hybrid molecules known as calixphyrins [8].

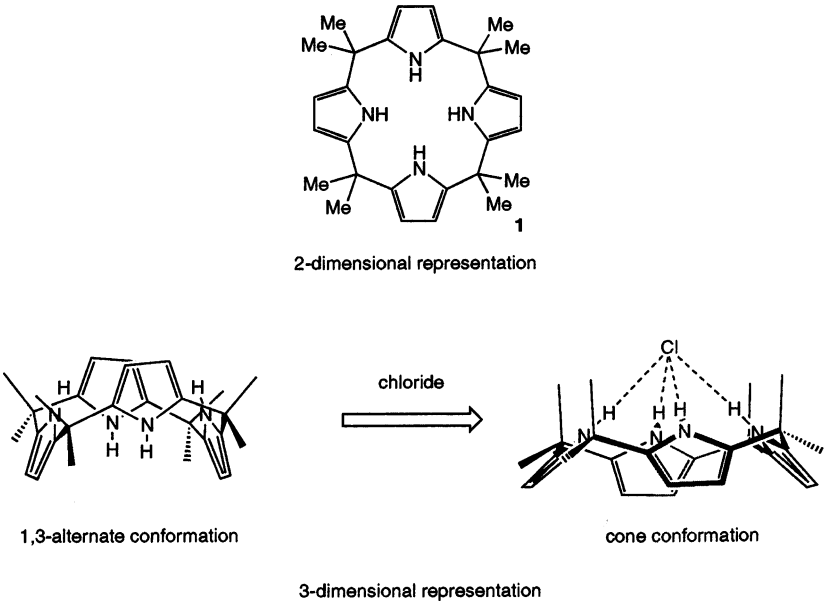

Scheme 1.

2. New synthetic methods

2.1. Modification at the C-rim

In 1997 we reported that reaction of *meso*-octamethylcalix[4]pyrrole with 4 equiv. of *n*-butyllithium followed by addition of ethyl bromoacetate resulted in mono- or poly-alkylation at β-pyrrolic sites, positions that are equivalently referred to as lying on the so-called *C*-rim of the calixpyrrole [9]. The conditions of this reaction were optimized in order to achieve the highest yield of mono-substituted calixpyrrole with the product isolated by column chromatography. *C*-rim substitution was confirmed by ^{1}H- and ^{13}C-NMR studies (mono-*C*-rim substitution leads to a complete loss of symmetry in the macrocycle and hence the number of β-pyrrole carbon resonances in the ^{13}C spectrum increases from one to eight. Recently, the crystal structure of the mono-ester **3** (Scheme 1) was obtained; it provides additional confirmation of *C*-rim substitution (Fig. 1).

The above, initially unexpected result led us to test the generality of the chemistry in question and to ask, in particular, whether it would be possible to prepare a range of *C*-rim substituted calix[4]pyrroles. Briefly, analogous synthetic procedures using carbon dioxide, iodine monochloride, *N*-formyl piperidine and 2-(2-bromoethoxy)-tetrahydro-2H-pyran as electrophiles proved successful and were used to prepare the acid **4**, iodo **5**, formyl **6** and protected alcohol **7** calix[4]pyrrole derivatives, respectively (Scheme 2) [10]. The yields and product distributions for these reactions are shown in Table 1.

Table 1
The effect of electrophile equivalents employed on isolated yield of monosubstituted calix[4]pyrrole derivatives. All syntheses were carried out using 4 mol. equiv. of *n*-BuLi except entry 5 (3.0 equiv.). Data taken from Ref. [10]

Entry	Product	Electrophile	Equivalents of electrophile	Yield (%) of monosubstituted product	Yield (%) of disubstituted derivatives
1	**3**	Ethyl bromoacetate	3	35	11
2	**3**	Ethyl bromoacetate	2	21	<5
3	**4**	Solid CO_2	Excess	17	<4
4	**5**	Chloroiodide (ICI)	2	13	<5
5	**5** [a]	Chloroiodide (ICI)	1	7	Traces
6	**6** [b]	*N*-Formyl piperidine	2	7	<3
7	**7**	2-(2-Bromoethoxy)-tetrahydro-2H-pyran	5	12 [c]	None detected

[a] Lithiation of the starting calix[4]pyrrole **1** was performed using only 3 equiv. of *n*-BuLi.

[b] Although higher yields of the formyl derivative **6** may be achieved by using 3 equiv. of *N*-formyl piperidine (yields up to 15%), such an enhanced yield is accompanied by an increased presence of unwanted doubly functionalized material (ca. 5–7%).

[c] Assumes deprotection of the intermediate tetrahydropyranyl derivative is quantitative.

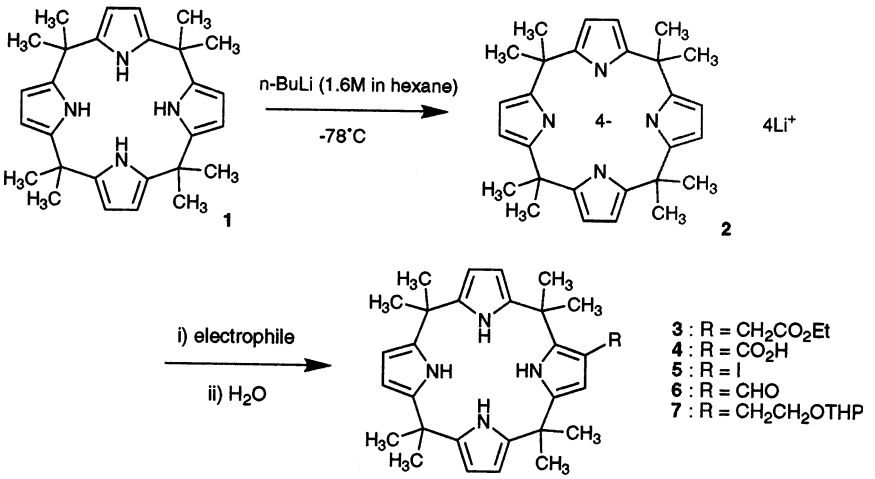

Scheme 2.

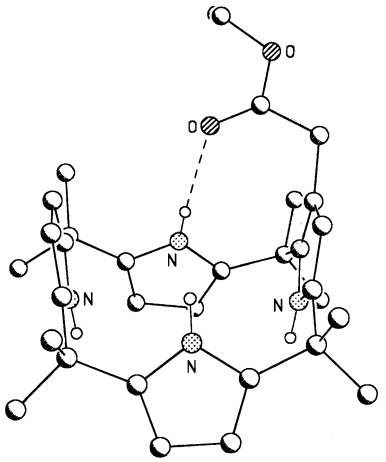

Fig. 1. The X-ray crystal structure of the calix[4]pyrrole mono-ester derivative **3**. Diagram produced using data from the Cambridge Crystallographic Database.

Crystals of the mono-acid derivative **4** and mono-formyl derivative **6** were obtained from solutions of the macrocycles in DMSO and dichloromethane–methanol, respectively. The crystal structure of the acid derivative confirms mono-β-substitution (Fig. 2) with the macrocycle adopting a partial cone conformation with three hydrogen bonds formed to one DMSO molecule and one hydrogen bond to another DMSO. The crystal structure of the formyl derivative **6** (Fig. 3) reveals the formation of a calixpyrrole-mediated dimer in the solid state bridged via NH···O=C hydrogen bonds. (Fig. 3).

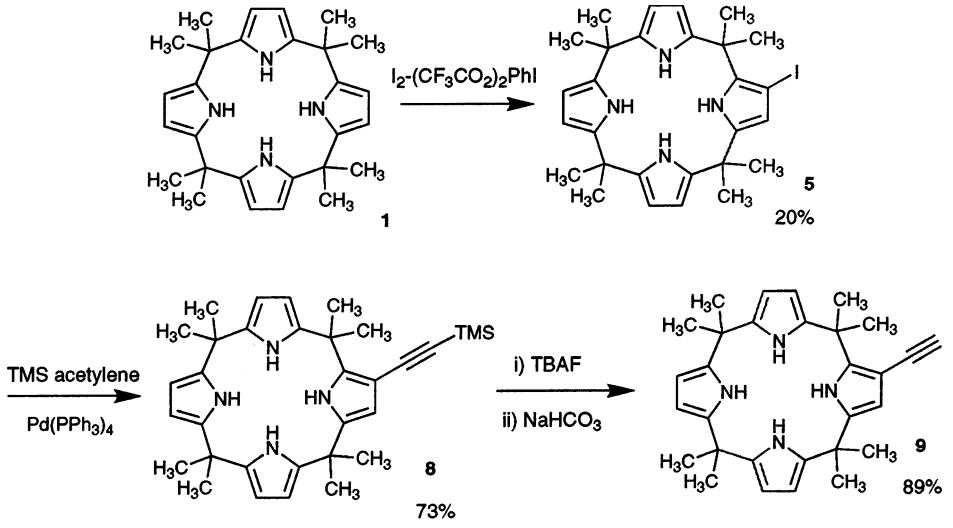

Scheme 3.

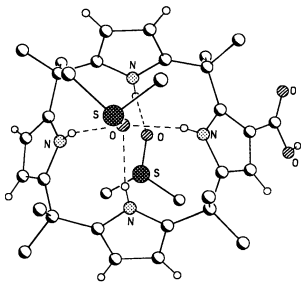

Fig. 2. The X-ray crystal structure of the calix[4]pyrrole mono-acid derivative **4**. Diagram produced using data from the Cambridge Crystallographic Database.

An alternative, higher yielding route to the mono-iodo derivative **5** and its subsequent conversion to mono-alkynyl derivatives has recently been reported [11]. Specifically, the mono-iodo derivative was obtained in 20% yield by reaction of the parent macrocycle with iodine-[bis(trifluoroacetoxy)iodo]benzene at room temperature (Scheme 3). Reaction of the mono-iodo derivative with TMS acetylene in diisopropylamine–DMF at 80°C in the presence of $Pd(PPh_3)_4$–CuI yielded the mono TMS acetylene derivative **8** in 73% yield. The crystal structure of this compound is shown in Fig. 4. This material could be deprotected by reaction with tetrabutylammonium fluoride then basic work-up to afford the mono-alkynyl derivative **9** in 89% yield. This material has served as a key precursor for the synthesis of calixpyrrole based anion sensors, as discussed later on in this review.

Palladium catalyzed coupling of compound **9** leads to the formation of a linear calixpyrrole dimer **10**, whilst a stepwise coupling with 1,3- or 1,4-diiodobenzene

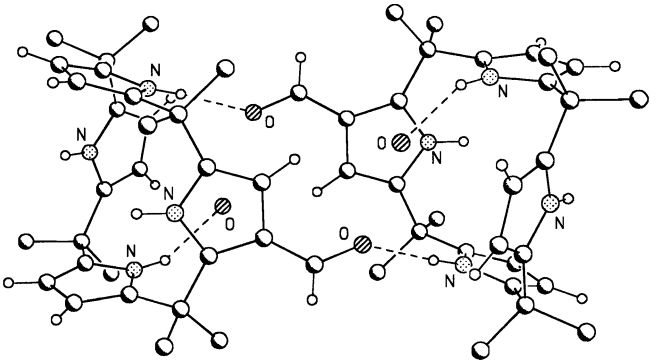

Fig. 3. The X-ray crystal structure of the calix[4]pyrrole mono-formyl derivative **6** that forms a dimer in the solid state via an N – H···O = C hydrogen bond. A water molecule is bound to each calix[4]pyrrole core. Diagram produced using data from the Cambridge Crystallographic Database.

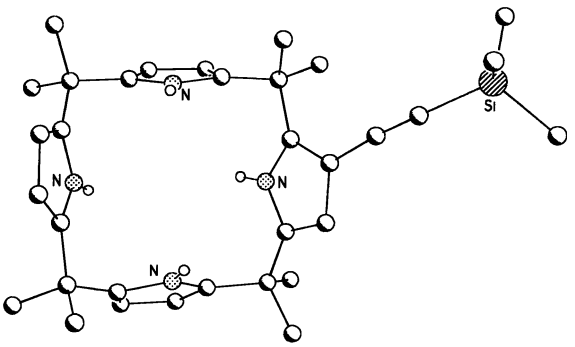

Fig. 4. The X-ray crystal structure of the calix[4]pyrrole mono-TMS acetylene derivative **8**. Diagram produced using data from the Cambridge Crystallographic Database.

leads, respectively, to the formation of the elongated calixpyrrole dimer **13** or the 'bent' dimer **14** (Scheme 4) [12].

The stoichiometry and association constants of aromatic dicarboxylate complexes of compound **10** have been determined using ^{1}H-NMR spectroscopic titration techniques (Table 2) [12]. A high selectivity for isophthalate anion was observed. This finding was rationalized in terms of the dianion forming a complex with both calix[4]pyrroles present in the dimer. As the two pyrrole rings linked by the alkynyl spacer are directed away from the anion binding site, hydrogen bond formation is only possible with six out of the possible eight pyrrole rings (Fig. 5). This is reflected in the ^{1}H-NMR spectrum with shifts of only six pyrrole NH groups being observed upon addition of isophthalate anion.

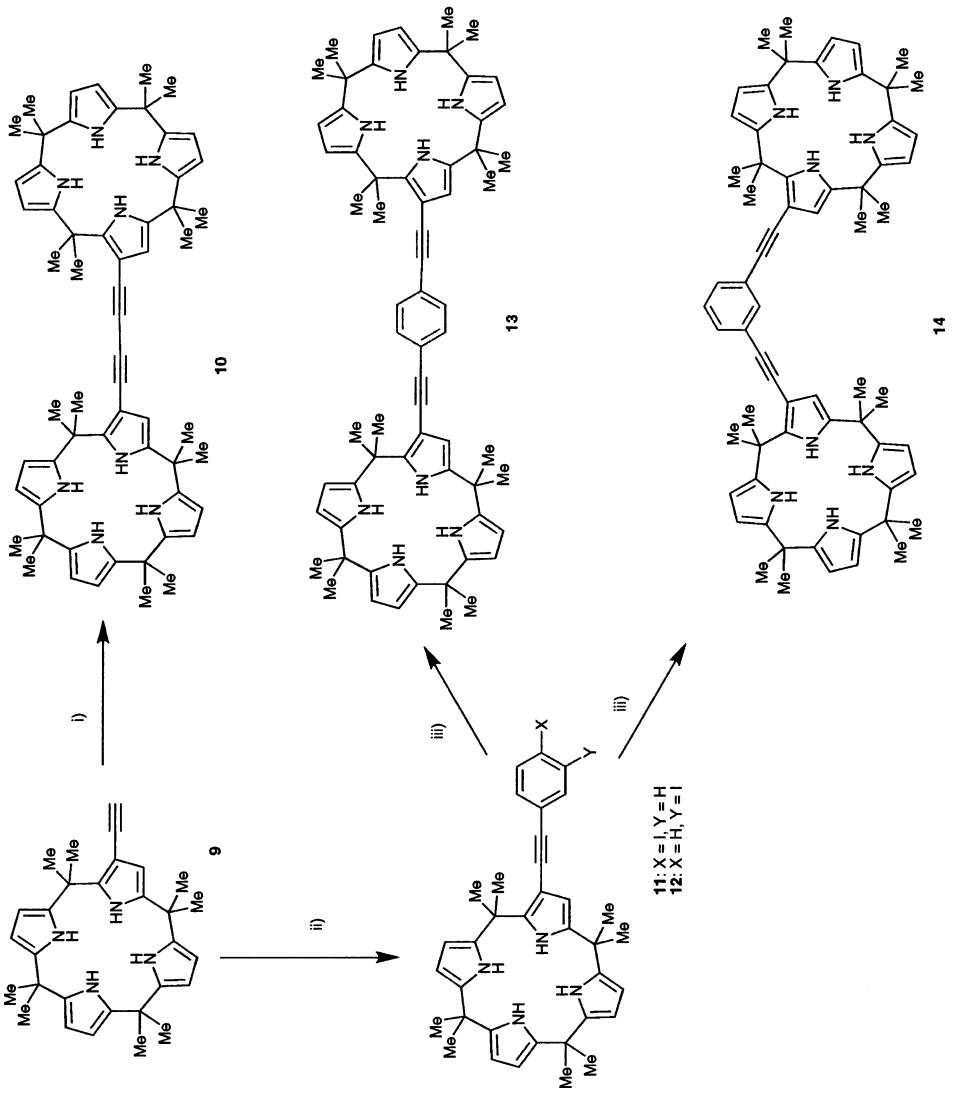

Scheme 4.

Table 2
Association constants [a] and binding stoichiometries for the interaction of dimer **10** and *meso*-octamethylcalix[4]pyrrole with aromatic carboxylate guests in CD_2Cl_2 at 298 K. Data taken from Ref. [12]

Anionic guest [b]	Dimer **10**		Compound **1**	
	K_a	Host:guest [c]	K_a	Host:guest [c]
Isophthalate	4180	1:1	700	1:1
Phthalate	$K_1 = K_2 = 90$	1:2	390	1:1
Benzoate	$K_1 = K_2 = 70$	1:2	230	1:1

[a] Estimated errors were $<15\%$.
[b] Anionic guests were added as their tetrabutylammonium salts.
[c] Stoichiometries were determined by Job plots.

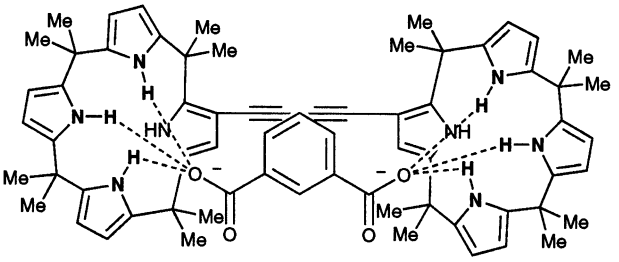

Fig. 5. Isophthalate binding in the calix[4]pyrrole dimer **10** involves only six of the eight pyrrole NH groups.

2.2. Modification at the N-rim

As discussed above, lithiation of calix[4]pyrrole and subsequent addition of an electrophile, results, under normal circumstances in the formation of a *C*-rim modified product. Takata and co-workers have recently reported a method for modifying the calix[4]pyrrole *N*-rim [13]. Reaction of *meso*-octaethylcalix[4]pyrrole **15** with sodium hydride and methyl iodide in the presence of 18-crown-6 in THF was found to give a distribution of N-methylated calixpyrroles **16**–**20**. The variation of product distribution with the concentration of MeI is shown in Table 3. When 1 equiv. of methyl iodide was used, the main product was the mono-N-methylated derivative **16**. However, when 2 equiv. were used, a higher proportion of the bis-, tris- and tetrakis-derivatives was observed with the 1,3-dimethylated derivative **18** being the major component. X-ray diffraction quality single crystals of **18** were obtained from toluene solution. The resulting structure revealed that the macrocycle adopts a 1,3-alternate conformation in the solid state (Fig. 6). Alkylation with ethyl iodide resulted in the isolation of the mono-ethyl derivative **21** only. The authors speculate that, in solution, reaction of calix[4]pyrrole **15** with butyl lithium results in the formation of a tight ion pair between the deprotonated calix[4]pyrrole nitrogen atoms and the lithium cations. Under their reaction conditions Takata and co-workers propose that the 18-crown-6 serves to break up this

Table 3
Distribution of products formed upon subjecting *meso*-octaethylcalix[4]pyrrole **15** to N-methylation

Reactant molar ratio MeI:**5**	Product distribution (%) [a]					Recovery (%)
	16	**17**	**18**	**19**	**20**	**15**
1:1	29	0.8	5.0	<1	<1	66
2:1	0.6(<1)	0.8(<1)	37(30)	23(13)	22(5)	17

[a] Product distributions were estimated on the basis of ^{1}H-NMR (500 MHz) spectral studies of the reaction mixtures. Isolated yields are given in parentheses. Data taken from Ref. [13].

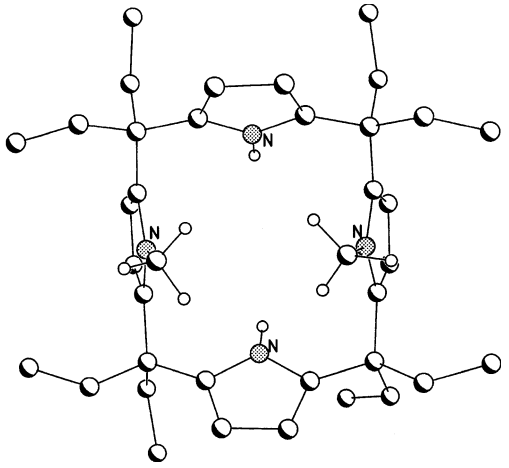

Fig. 6. The X-ray crystal structure of the 1,3-*N*-dimethylated calix[4]pyrrole derivative **18**. Diagram produced using data from the Cambridge Crystallographic Database.

ion pair, thereby allowing N-alkylation to occur. While far from proven, important support for this hypothesis comes from the solid state structural analyses of Floriani [14]; in the case of tetralithio-*meso*-octaethylcalix[4]pyrrole these latter researchers observed an ion pair analogous to that proposed by Takata.

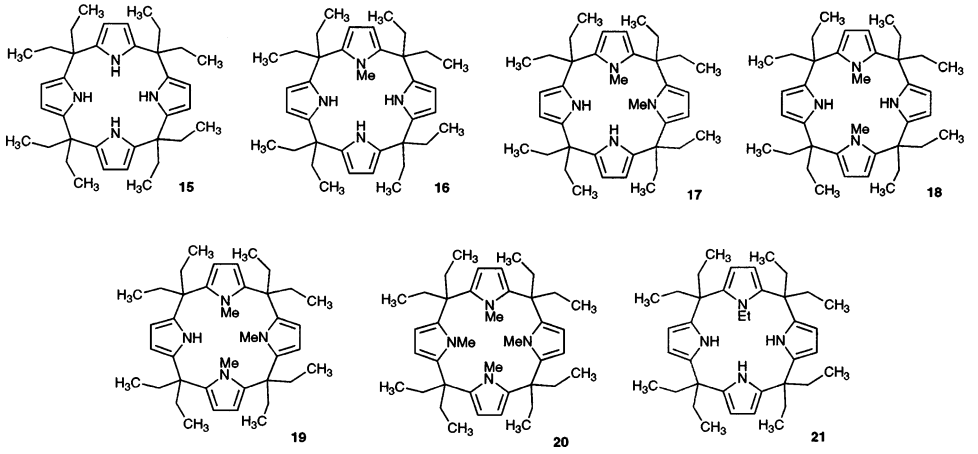

2.3. Modification at the meso-position

Our earliest efforts at synthesizing functionalized calix[4]pyrroles were directed towards producing *meso*-functionalized derivatives by condensing mixtures of different ketones with pyrrole. Subsequent chromatographic separation then yielded the desired mono-functionalized derivative [15]. We have recently revisited this approach and used it to produce amine functionalized calixpyrroles [16]. Specifically, condensation of Cbz-protected 3-aminoacetophenone, 3-pentanone and pyrrole in the presence of $BF_3{\cdot}Et_2O$ was found to afford the mono-functionalized calix[4]pyrrole **22**. Subsequent deprotection by Pd–C gave the mono-amine functionalized calixpyrrole **23** in 21% overall yield (Scheme 5). This latter product has seen application as a synthetic precursor to fluorescent calix[4]pyrrole anion sensors, as discussed below.

3. Modeling studies

van Hoorn and Jorgensen [17] have investigated the anion selectivities of calix[4]pyrroles using Monte Carlo simulations. In agreement with the experiment [2], they found that of the four possible conformations (cone, partial cone, 1,3-alternate and 1,2-alternate) the 1,3-alternate conformer of calix[4]pyrrole was most stable in the absence of anions, whilst the cone conformer was the most stable conformation when the calix[4]pyrrole was bound to a halide anion. Free energy calculations on the binding of chloride, bromide and iodide in dichloromethane were found to be in excellent agreement with experiment. However, the affinity of calix[4]pyrrole for fluoride anions was predicted to be higher than that observed by the experiment. This disparity was attributed to the presence of trace quantities of water in the samples used to determine the fluoride anion association constants via standard ^{1}H-NMR spectroscopic titration methods.

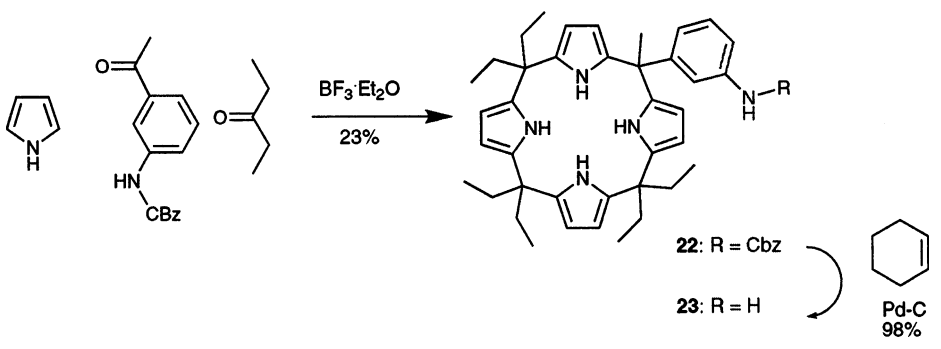

Scheme 5.

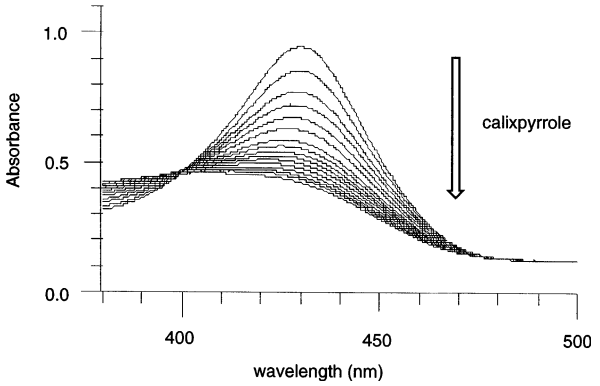

Fig. 7. Decrease in the absorbance of the 4-nitrophenolate anion **24** (3.6×10^{-5} mol dm^{-3}) observed upon the addition of calixpyrrole **1** (5×10^{-2} mol dm^{-3}) in dichloromethane at 25°C. (Reproduced with permission from Chem. Commun. (1999) 1851, Copyright 1999, The Royal Society of Chemistry.)

4. Calixpyrrole based optical sensors

The synthesis of new molecular devices designed to sense and report the presence of a particular substrate is an area of analytical chemistry that is attracting intense current interest. Two main approaches have been used in the production of calix[4]pyrrole based optical anion sensors. The first of these is based on the covalent attachment of a colorimetric or fluorescent reporter group to the calix[4]pyrrole skeleton. Perturbation of the electronic properties of these reporter groups upon anion complexation then produces a response detectable by visual or fluorescence-based means. The second strategy centers around the use of a displacement assay [18]. In this scenario, an initial calix[4]pyrrole complex involving a colored anion is used that becomes broken up upon the addition of a more strongly coordinating anionic analyte. These approaches are shown schematically in Scheme 6.

The second, displacement-based approach has been explored less extensively than the first. Still, this strategy has been exploited successfully to produce a very simple but effective colorimetric halide sensor system [19]. Specifically, it was discovered that the 4-nitrophenolate anion **24** loses its intense yellow color when bound to *meso*-octamethylcalix[4]pyrrole **1** (Fig. 7). This allows the calix[4]pyrrole–4-nitrophenolate complex **1**–**24** to be used as a colorimetric displacement assay (Scheme 7). Anions, such as fluoride, displace the 4-nitrophenolate anion from the complex thereby restoring the native absorbance of the 4-nitrophenolate anion. This was observed as a colorless to yellow color change, with the intensity of the recovered yellow color being both a relative and absolute measure of the affinity of calix[4]pyrrole for the analyte anion (Fig. 8).

A number of covalently linked, calixpyrrole-based optical sensor systems have been synthesized in the last two years. The first generation systems consisted of anthracene groups attached to the calix[4]pyrrole skeleton via amide bonds [20].

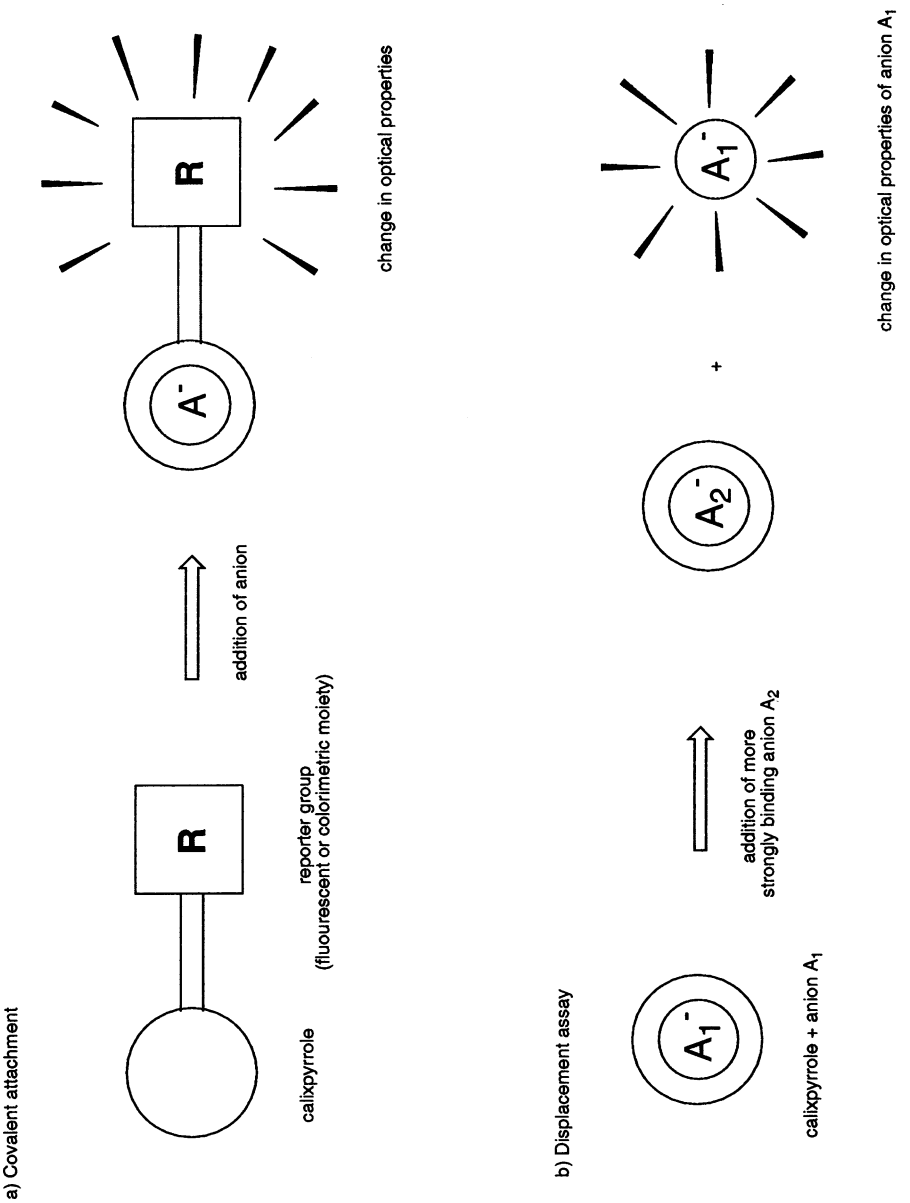
a) Covalent attachment
R
calixpyrrole
reporter group
(fluourescent or colorimetric moiety)
addition of anion
A-
R
change in optical properties
b) Displacement assay
A1-
calixpyrrole + anion A1
addition of more
strongly binding anion A2
A2-
+
A1-
change in optical properties of anion A1

Scheme 6.

For example, the mono-acid derivative **4** was coupled to 1-aminoanthracene using dicyclohexylcarbodiimide (DCC) and hydroxybenzotriazole (HOBt) in DMF to afford a calix[4]pyrrole–anthracene conjugate **25** (in 34% yield from the acid) that possesses a direct link between the calix[4]pyrrole anion binding site and the anthracene fluorophore. Other calix[4]pyrrole–anthracene conjugates were synthesized by coupling the calix[4]pyrrole mono-acid derived by saponification of compound **3** with 1-aminoanthracene or 9-aminomethylanthracene using the benzotriazolyloxy-tris(dimethylamino)phosphonium (BOP) amide coupling reagent. This afforded the conjugate compounds **26** and **27** in 63 and 51% yields, respectively.

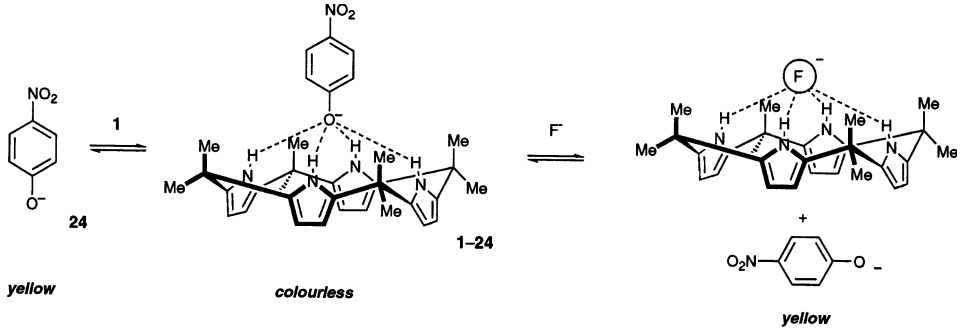

Scheme 7.

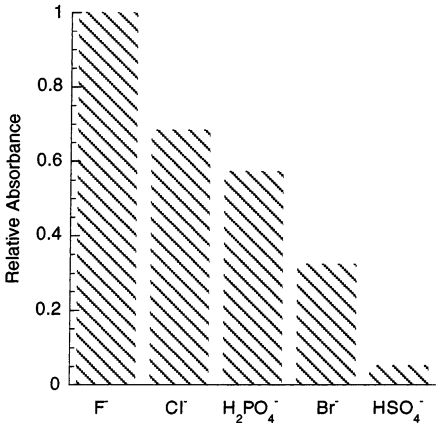

Fig. 8. Relative absorbance of solutions containing **1** (5.0×10^{-4} mol dm^{-3}), **24** (6.0×10^{-6} mol dm^{-3}) and various anions (1.6×10^{-2} mol dm^{-3}) in acetonitrile at 25°C.

Table 4
Association constants of compounds **25**, **26** and **27** with various anions in the form of their tetrabutylammonium salts, as determined from ^{1}H-NMR spectroscopic titrations carried out in acetonitrile-d_3. Errors < 15%. Data taken from Ref. [20]

Anion	Association constant (log K_a) of compound **25** in CD_3CN	Association constant (log K_a) of compound **26** in CD_3CN	Association constant (log K_a) of compound **27** in CD_3CN
F^-	[a]	[a]	[a]
Cl^-	>4	>4	>4
Br^-	3.59	3.00	2.63
$H_2PO_4^-$	>4 [b]	3.50	3.08
HSO_4^-	2.77	[c]	[c]

[a] NH resonance broadened precluded a determination of this value using ^{1}H-NMR spectroscopic methods.
[b] Association constant determined by following pyrrole CH resonance.
[c] Weak interaction $K_a < 20$ mol^{-1} dm^3.

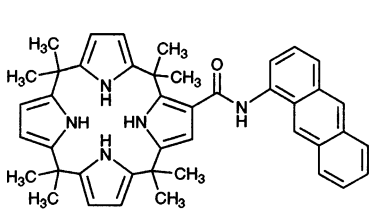

25

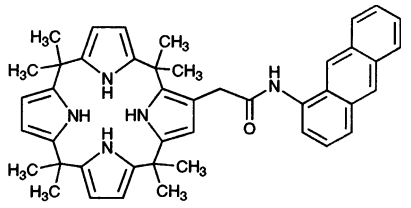

26

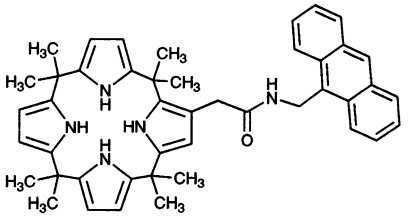

27

Compounds **25**, **26**, and **27** represent a "matched set" containing linkers of increasing length (i.e. with zero, one or two methylene groups between the calix[4]pyrroles and anthracene fluorophores). Association constants for anion binding were determined in acetonitrile-d_3 using standard ^{1}H-NMR spectroscopic titration techniques (Table 4). The fluorescence of receptors **25**, **26**, and **27** was shown to be quenched significantly in the presence of certain anionic guests (most efficiently by fluoride). It was also found that of the three compounds, receptor **25** was most sensitive, having its fluorescence quenched most efficiently by the added anions. This added sensitivity is thought to reflect the electron withdrawing effect of

the directly linked amide group, as well as the possibility for direct electronic conjugation between the anion binding site and the fluorophore. The changes in the fluorescence spectrum of compound **25** induced upon the addition of fluoride anions are reproduced in Fig. 9.

A series of 'second generation' calix[4]pyrrole anion sensors **28**, **29**, and **30** based upon the *meso*-mono-amine calix[4]pyrrole **23** core (see Section 2.3 above) have been produced. These incorporate a second anion binding site (either an amide or thio-urea group) in conjunction with a fluorescent reporter group (dansyl, Lissamine™-rhodamine B or fluorescein) [16]. The presence of the second anion-binding group alters the anion selectivity of the calix[4]pyrrole as the calix[4]-

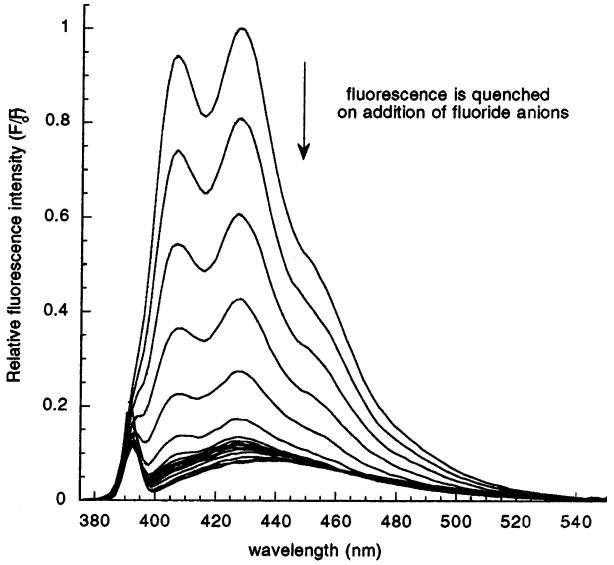

Fig. 9. Fluorescence spectra of calix[4]pyrrole **25** in CH_2Cl_2 (5×10^{-5} mol dm^{-3}) showing the changes induced upon the addition of increasing quantities of tetrabutylammonium fluoride. (Reproduced with permission from Chem. Commun. (1999) 1723, Copyright 1999, The Royal Society of Chemistry.)

Table 5
Association constants (mol^{-1} dm^3) for sensors **28**–**30** and anionic substrates as determined by emission quenching in acetonitrile (0.01% v/v water) for sensors **28** and **29** and acetonitrile–water (96:4, pH 7.0 ± 0.1) for sensor **30**. Data taken from Ref. [16]

Anion	Sensor		
	28	**29**	**30**
F^-	222,500	>1,000,000	>2,000,000
Cl^-	10,500	18,200	<10,000
$H_2PO_4^-$	168,300	446,000	682,000
$HP_2O_7^{3-}$	131,000	170,000	>2,000,000

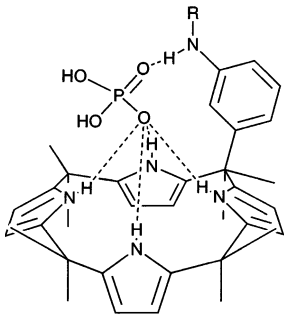

Fig. 10. Representation of the interaction between calix[4]pyrroles **28**, **29** and **30** and phosphate anions that is proposed to account for the increased affinity of these receptors for phosphate-type anions.

pyrrole–amide or calix[4]pyrrole–thiourea conjugate is effectively now a ditopic receptor. Specifically, selectivity is enhanced for dihydrogenphosphate and pyrophosphate relative to chloride (Table 5).

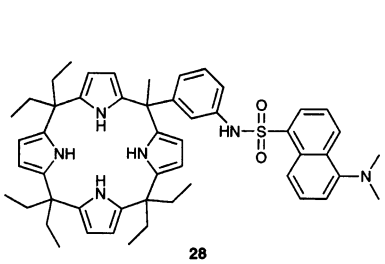

28

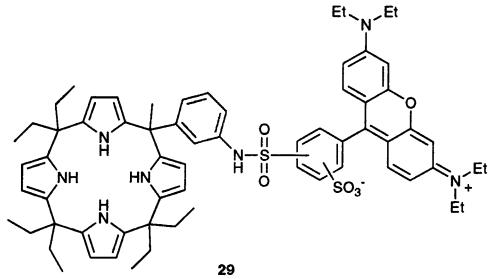

29

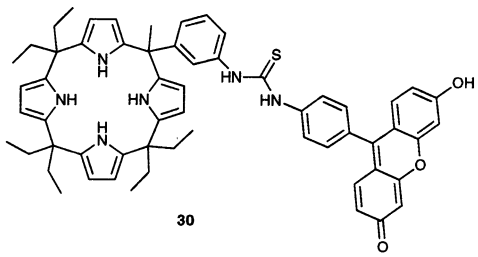

30

The increased affinity for phosphates is attributed to a pseudo 'two-point' interaction between the receptor and the bound anion, a mode of binding which is not possible with the smaller chloride anion (Fig. 10).

The fluorescence of receptors **28**, **29**, and **30**, all three of which function as very effective sensors, were found to be quenched in the presence of anions. By way of example, the decrease in fluorescence emission intensity observed when receptor **29** is titrated with an increasing concentration of fluoride anion is illustrated in Fig. 11.

The mono-alkynyl calix[4]pyrrole derivative **9** has also been used as a basis for the construction of optical anion sensing agents [11,21]. Palladium catalyzed

coupling of a variety of aromatic species including nitroaromatics, anthraquinones and pyrene with **9** have afforded a new library of calix[4]pyrrole derivatives **31**–**38** (Scheme 8). The anion sensing potential of these compounds is illustrated in Fig. 12 which shows the red-shift and broadening in the absorption spectrum of compound **33** in dichloromethane observed upon the addition of fluoride anions (in fact λ_{max} shifts from 441 to 498 nm in this case). As a consequence of this anion-induced perturbation in the absorption spectrum, a naked eye-detectable color change from yellow to red is observed. Compound **31**, displaying a λ_{max} at 308 nm in dichloromethane, is colorless and was used as a control in these studies. Addition

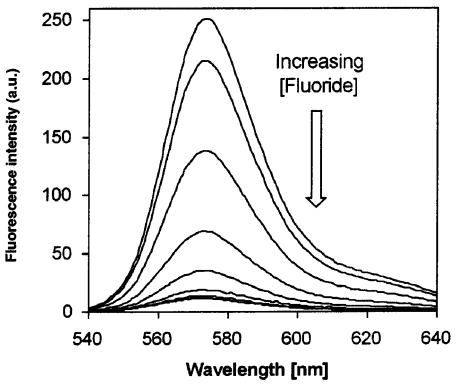

Fig. 11. Fluorescence spectra of calix[4]pyrrole **29** in CH_2Cl_2 showing the changes induced upon the addition of increasing quantities of tetrabutylammonium fluoride.

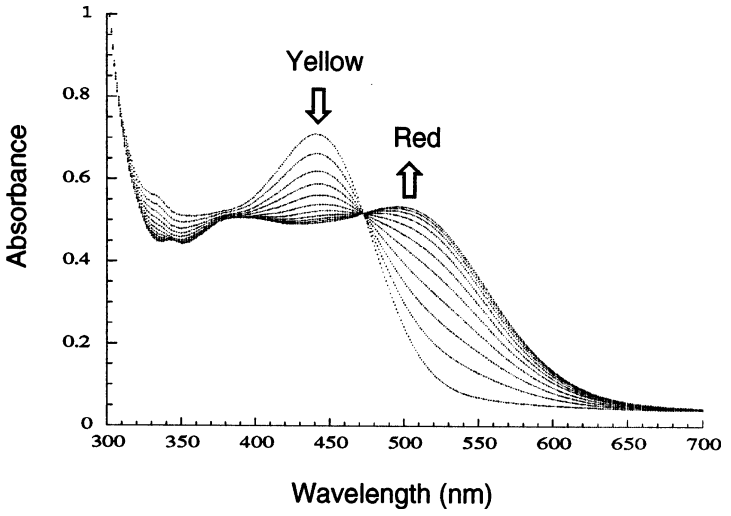

Fig. 12. Absorption spectra of calix[4]pyrrole **33** recorded in CH_2Cl_2 (5.0×10^{-5} mol dm^{-3}) before and after the addition of 0.2, 0.4, 0.6, 0.8, 1, 1.2, 1.4, 1.6, 1.8, and 2 equiv. of tetrabutylammonium fluoride. (Reproduced with permission from Tetrahedron Lett. 41 (2000) 1369, Copyright 2000, Elsevier.)

ArI
[Pd(PPh3)4], CuI
9
31: Ar =
87%
32: Ar =
82%
33: Ar =
67%
34: Ar =
81%
35: Ar =
79%
36: Ar =
73%
37: Ar =
82%
38: Ar =
69%

Scheme 8.

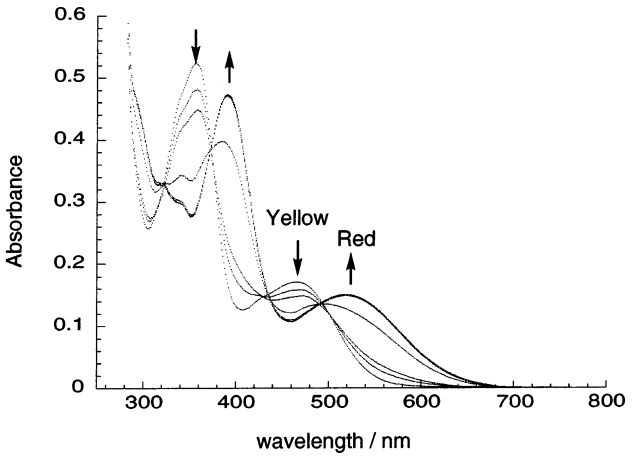

Fig. 13. Absorption spectra of calix[4]pyrrole **36** recorded in CH_2Cl_2 (5.0×10^{-5} mol dm^{-3}) after the addition of 0, 1, 2, 4, 6, 8, and 10 equiv. of tetrabutylammonium fluoride. (Reproduced with permission from Angew. Chem. Int. Ed. Engl. 39 (2000) 1777, Copyright 2000, Wiley–VCH.)

of 20 equiv. of fluoride to solutions of this latter compound lead to only a small shift in λ_{max} (specifically, to 321 nm). On the other hand, the presence of the nitro-groups in **33** produces a naked eye detectable bathochromic shift in the presence of certain anions with larger shifts being observed in the case of the more tightly bound anions (e.g. F^-). These observations are rationalized in terms of charge transfer between the bound anion and the electron deficient nitro-aromatic, with the alkynyl group acting as a conducting molecular wire [11].

Particularly dramatic color changes are observed with the anthraquinone derivatives **36** and **37** [21]. Compound **36** shows a clear yellow to red color change in the presence of fluoride and a slightly less intense change to orange/red when exposed to chloride and dihydrogen phosphate anions. The changes in the absorption spectrum of compound **36** observed upon the addition of fluoride anion are shown in Fig. 13.

The presence of an extra hydroxyl group in compound **37** 'color-tunes' the receptor with the response to appropriate anionic analytes now being observed as a dramatic red to blue or red to purple changes. As in the case of other receptors, the effect is most pronounced for fluoride anion. The absorption spectra of compound **37**, recorded in the presence of 100 mol equiv. of various anions, are reproduced in Fig. 14.

5. Calixpyrrole based electrochemical sensors

The development of electrochemical sensors for anions, based on calix[4]pyrroles has, just as for the optical sensors, proceeded via a number of different approaches. These include the incorporation of calixpyrroles in ion-selective electrodes, discrete electrochemically active receptors and chemically modified electrodes.

5.1. Ion-selective electrodes

PVC based ion-selective electrodes have been prepared [22] containing *meso*-octamethylcalix[4]pyrrole **1** and from calix[4]pyrrole analogues containing pyridine rings [23] i.e. dichlorocalix[2]pyrrole[2]pyridine **39** and tetrachlorocalix[4]pyridine **40**. At low pH values (e.g. pH 3.5 or 5.5), PVC derived ion selective electrodes containing **1** displayed strong anionic responses toward Br^-, Cl^- and $H_2PO_4^-$ and to a lesser extent F^-. However, at high pH, specifically pH 9.0, the calixpyrrole containing ISEs display non-Hofmeister selectivities ($Br^- < Cl^- < OH^- \approx F^- < HPO_4^{2-}$). Based on these observations and other evidence, it was concluded that at low pH the calixpyrrole macrocycles act as anion binding agents whereas at higher pH they coordinate hydroxide anions and show responses reflecting both anion binding and anionic analyte counter cation attraction. For the membranes derived from **39** and **40**, no non-Hofmeister selectivity was observed at pH 9.0, as proved the case for membranes derived from **1**. However, at lower pH, increased responses to hydrophilic anions (e.g. $H_2PO_4^-$ and F^-) are observed, along with generally improved anionic responses. These observations are considered consistent with the protonation of the pyridine heterocycles occurring to produce receptors in the PVC membrane that contain both positive charges and pyrrole-derived hydrogen bond donor sites [22].

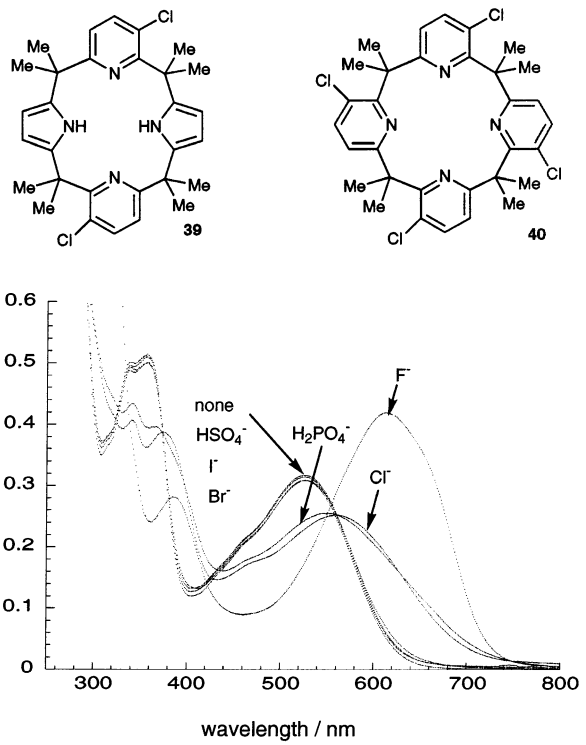

Fig. 14. Absorption spectra of **37** recorded in CH_2Cl_2 (5.0×10^{-5} mol dm^{-3}) after the addition of 100 equiv. of representative anions. (Reproduced with permission from Angew. Chem. Int. Ed. Engl. 39 (2000) 1777, Copyright 2000, Wiley–VCH.)

5.2. Discrete redox-active molecular receptors

The development of discrete redox-active receptors containing a guest binding site coupled to a redox-active reporter group is an area of supramolecular chemistry that has attracted much attention recently [24]. As a new part of this established area of research, it was considered worthwhile to append a redox-active ferrocene group to the calixpyrrole framework. This, it was thought, would allow the solution phase anion binding properties of the resulting receptors to be studied using electrochemical means [25]. Towards this end, compounds **41** and **42** were prepared by coupling the corresponding calix[4]pyrrole mono-acid species to aminomethylferrocene using the BOP amide coupling reagent.

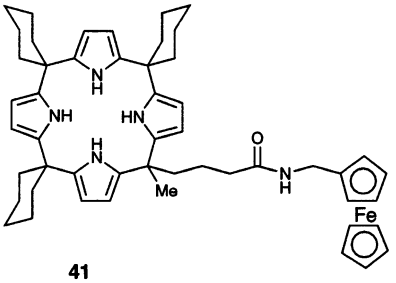

41

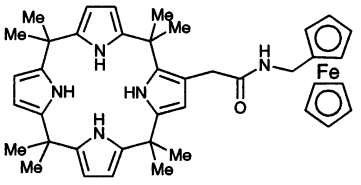

42

The association constants of **41** and **42**, elucidated using ^{1}H-NMR spectroscopic titration methods, are summarized in Table 6. Measurements were hampered in the case of compound **42** by a broadening of the pyrrole-NH and -CH signals during the course of the titration. Thus, unfortunately, a reliable association constant for fluoride anion could not be determined. Nonetheless, at least in the case of **41**, the expected affinity series $F^- > Cl^- > H_2PO_4^-$ could be unequivocally inferred.

The electrochemical properties of **41** and **42** were investigated using cyclic voltammetry (CV). The CV of β-ferrocenylamidocalix[4]pyrrole **41**, scanned between $+600$ and -100 mV, is shown in Fig. 15; it reveals a reversible ferrocene/ferrocenium wave ($E_{1/2} = 511$ mV vs. Ag/AgCl). However, when the CV is scanned between $+1.8$ and -1.8 V, further less reversible oxidation features are observed that are assigned to calix[4]pyrrole-centered oxidation processes. In this scanning

Table 6
Association constants for compounds **41** and **42** with anionic substrates in dichloromethane at 298 K and electrochemical parameters obtained from CV measurements carried out in the absence and presence of anions

Anion [a]	Receptor **41**			Receptor **42**		
	K_a (mol^{-1} dm^3) [b]	$E_{1/2}$ (mV) [c]	ΔE (mV) [d]	K_a (mol^{-1} dm^3) [b]	$E_{1/2}$ (mV) [c]	ΔE (mV) [d]
No anion	N/A	511	N/A	N/A	503 mV	N/A
Dihydrogen phosphate	40 [e]	502	−9	40	534	31
Fluoride	[f]	525	14	1496	566	63
Chloride	202	718	207	444	481	−22

[a] Used in the form of their $(n\text{-}Bu_4N)^+$-salts.
[b] Association constants for anion binding; recorded in dichloromethane-d_2 errors $<20\%$; determined from $\Delta(\delta)$ (ppm) N*H*.
[c] Determined in dichloromethane containing 0.1 mol dm^{-3} (n-Bu_4NPF_6) as the supporting electrolyte. Solutions of 41/42 were 5×10^{-4} mol dm^{-3} and potentials were determined with reference to Ag/AgCl.
[d] Shifts determined by square wave voltammetry.
[e] This value was determined using the chemical shift of the β-CH of the pyrrole since the pyrrole-NH signal became too broad to be followed accurately during the titration.
[f] NMR signals became very broad in this case so that an accurate determination of this value was impossible.

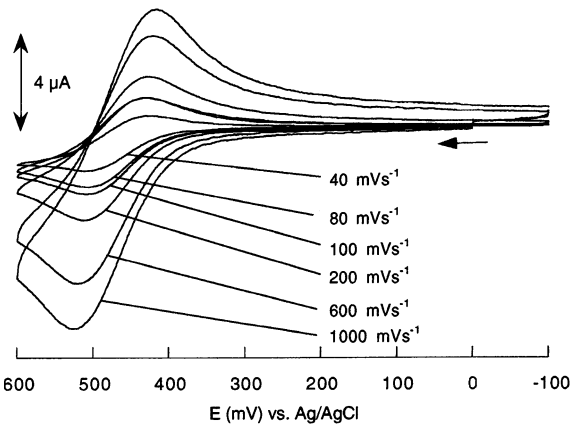

Fig. 15. The cyclic voltammogram of **41** recorded in CH_2Cl_2 at various scan rates (0.1 M n-Bu_4NPF_6).

window, the Fc/Fc^+ couple becomes quasi-reversible, presumably due to electrochemical coupling to the redox-active calix[4]pyrrole moiety. Compound **42** behaves in a similar manner.

The arrangement of the calixpyrrole anion binding site and ferrocene group led to the reasonable expectation that in both compounds **41** and **42** a cathodic shift in the ferrocene/ferrocenium redox wave would occur as an analyte anion was bound.

However, surprisingly, both anodic and cathodic shifts were observed upon the addition of anions (Table 6). Cathodic shifts of **14** and 207 mV were observed for the Fc^+/Fc couple of β-ferrocenylamidocalix[4]pyrrole 41 upon addition of fluoride and chloride anions, respectively. However, the addition of dihydrogenphosphate anions to this system was found to lead to an *anodic* shift of -9 mV (Table 6). An anodic shift in the Fc^+/Fc couple was also seen when chloride anions were added to **42**. By contrast, the Fc/Fc^+ couple is found to be *cathodically* shifted upon the addition of dihydrogenphosphate (31 mV) and fluoride (63 mV) anions. It is clear that significant electrochemical effects are caused by the addition of certain anions; however, the direction of the shifts observed are such that no clear rationalization of the anion-induced response can be put forward at the present time.

5.3. Chemically modified electrodes

As discussed above, one way of utilizing calixpyrroles in the production of modified electrodes is to incorporate the macrocycles into a PVC based membrane to produce an ion-selective electrode. An alternative route to the production of a modified electrode is by the production of an electropolymerized matrix formed from a receptor bound to an electropolymerized moiety [26]. Pyrrole rings that do not carry substituents in the 2- and 5-positions are known to form electropolymerized films via either potential cycling or chronoamperometry. Bearing this in mind, chemically modified electrodes were prepared from calix[4]pyrrole monomers containing α-unsubstituted pyrrole moieties [27]. Here, the requisite α-unsubstituted pyrrolic species, compounds **43** and **44** (Scheme 9), were synthesized using methods analogous to those used to prepare **41** and **42**. Specifically, they were made by coupling the relevant calix[4]pyrrole mono-acid species with 3-aminopropylpyrrole using the BOP amide coupling agent.

Once **43** and **44** were in hand, initial attempts to effect polymerization were made using cyclic voltammetric (potential cycling) methods. Unfortunately this method did not produce a conducting polymer, as judged from the fact that current waves prior to monomer oxidation were not seen to increase with the number of cycles.

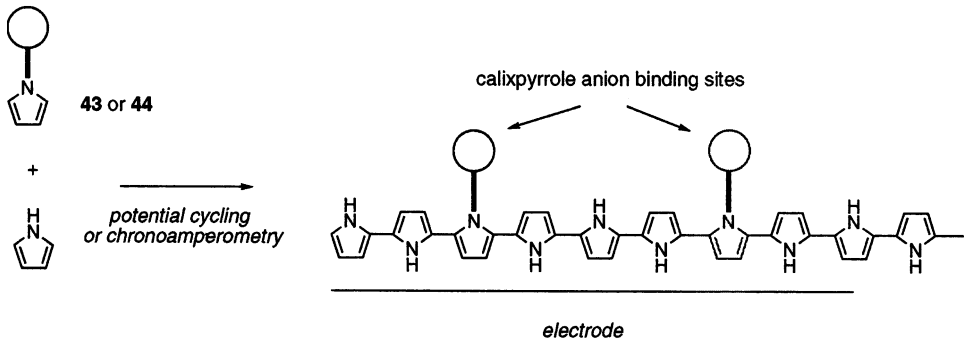

Scheme 9.

Instead, the current of both forward and backward potential scans was seen to decrease with each consecutive cycle. Attempts at using controlled potential electrolysis to generate the desired film also failed. Presumably, unfavorable steric interactions, associated with N-substitution, are serving to preclude film growth.

In order to reduce any potential steric interactions, polymerization of the calixpyrrole monomers was attempted in the presence of pyrrole. Under such polymerization conditions, the pyrrole subunits may act as spacers, increasing the distance between the calix[4]pyrrole macrocycles in the film, thereby allowing polymerization to occur (Scheme 9). The CVs recorded during potential cycling in a mixed solution of **43** + pyrrole and **44** + pyrrole are shown in Fig. 16a and b, respectively. These voltammograms are indicative of the in situ generation of a conducting polymer matrix (an increasing current is observed for each consecutive scan).

To confirm that co-polymerization of pyrrole and calixpyrrole had indeed occurred, CVs of the presumed co-polymer were compared to those obtained from a solution containing an equivalent concentration of pyrrole. It was found that both a higher initial oxidation current and a faster current increase with the number of cycles were observed in the case of the mixed polymer system, results that are consistent with the participation of the calix[4]pyrrole subunits in the polymerization process. In other words, the CVs recorded from the mixture of pyrrole and calixpyrrole reflect directly the co-polymerization of monomers.

To investigate the use of this co-polymer film in sensing anions, modified electrodes coated with either simple polypyrrole or the co-polymer were immersed in solutions of supporting electrolyte (0.1 mol dm^{-3}) containing tetrabutylammonium salts of various anions at concentrations at least an order of magnitude lower than the supporting electrolyte. It was found that for simple polypyrrole, when the electrode was immersed in a solution of the electrolyte containing tetrabutylammonium fluoride (5×10^{-4} mol dm^{-3}) the polymer redox waves shifted continuously to more positive potentials with the number of cycles. The same anion effect was observed in the co-polymer films of **43**-pyrrole and **44**-pyrrole. This effect masks any perturbation due to the formation of calix[4]pyrrole–anion complexes on the cyclic voltammogram. Work is planned to study the co-polymer films by other methods including spectroscopic, potentiometric and impedance techniques.

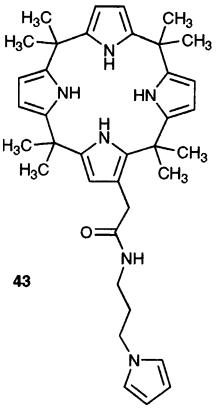

43

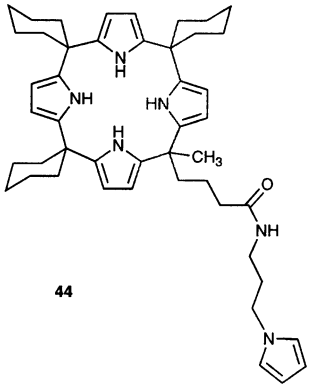

44

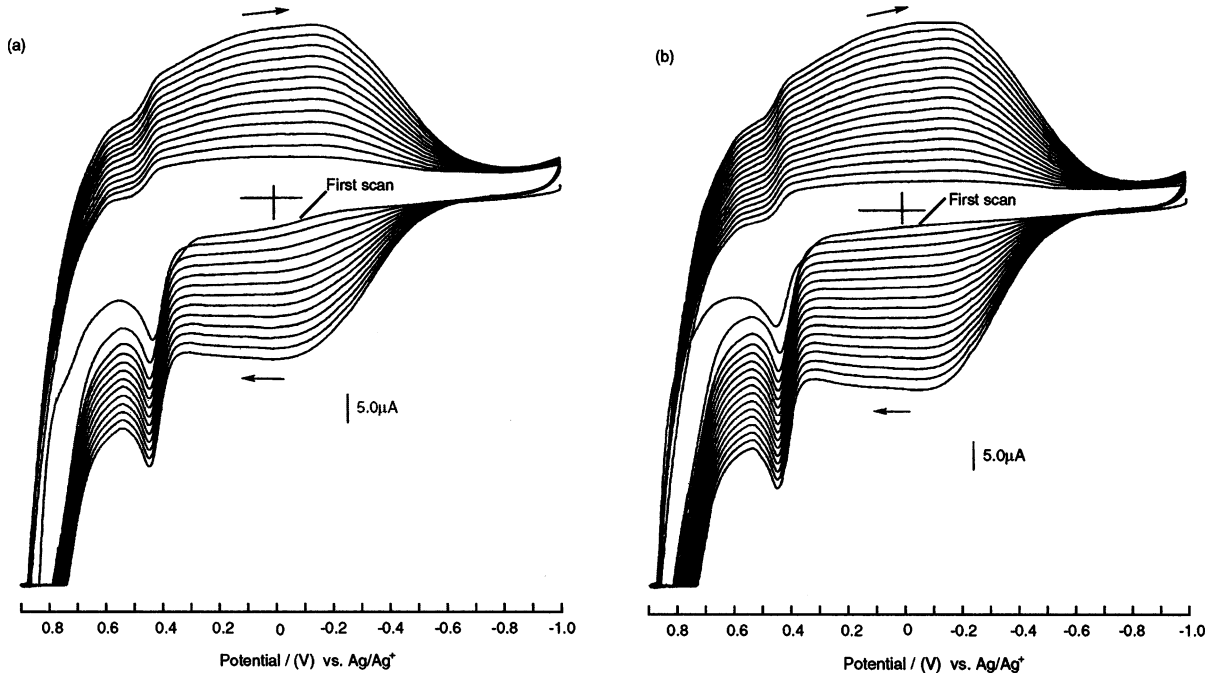

Fig. 16. Consecutive CVs of: (a) 5×10^{-4} mol dm^{-3} **43** and 5.0×10^{-4} mol dm^{-3} pyrrole; and (b) 5×10^{-4} mol dm^{-3} **44** and 5.0×10^{-4} mol dm^{-3} pyrrole in CH_3CN, scan rate 50 mV s^{-1}.

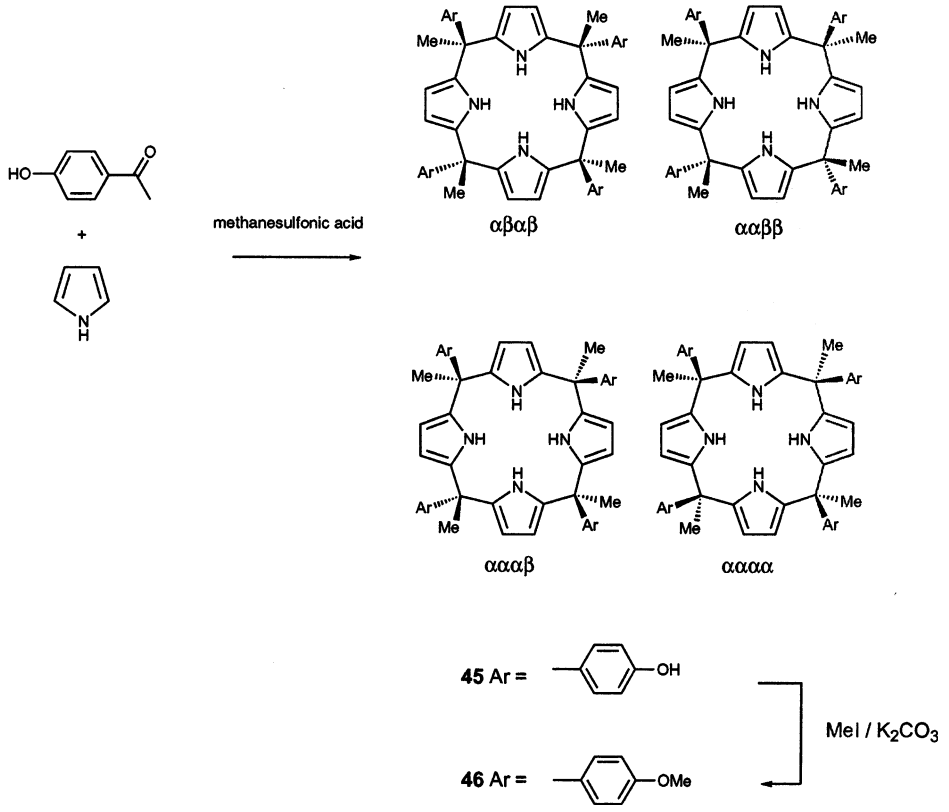

Scheme 10.

6. Extended cavity calix[4]pyrroles

In an effort to improve further the selectivity of calixpyrrole derivatives for particular anions and especially the chloride-over-phosphate selectivity (an important consideration for biological applications in which phosphate is present in high concentration and fluoride is absent), calix[4]pyrrole systems bearing substituted aryl groups in the *meso*-positions were prepared and their anion coordination properties examined [28]. The rationale for this work derives from the fact that the aryl groups alter the steric environment around the calixpyrrole anion binding site while also serving to alter the electronic properties of the macrocycle. This latter effect, in particular, has previously been shown to modulate the anion binding affinities of calix[4]pyrroles [29].

The synthetic procedure used to prepare *meso*-tetraarylcalix[4]pyrrole is shown in Scheme 10. Briefly, acid-catalyzed condensation of pyrrole and 4-hydroxyacetophenone provides a mixture of four configurational isomers that, in accord with the

porphyrin literature, are denoted as αβαβ, ααββ, αααβ and αααα to indicate the relative position of the bulky aryl substituents. The configurational isomers of **45** could be isolated cleanly using chromatographic methods, a result that reflects the marked differences in overall dipole moment of this isomeric set of tetraarylcalix[4]pyrrole molecules (Table 7).

Isomers of **45** were found to possess high walls and/or well-defined binding cavities, as judged from both solution phase NMR spectral analyses and solid state X-ray structural determinations (Fig. 17) [28,30]. Similar systems, including those formed by the condensation of 3-hydroxyacetophenone with pyrrole were also prepared contemporaneously by Floriani and co-workers [30]. As noted by these latter researchers, the arrangement of the four phenol groups in these compounds is reminiscent of the structure of calix[4]arene.

Not surprisingly, the presence of the well-defined binding cavity resulted in a greatly augmented selectivity for fluoride anion, relative to chloride anion and phosphate. Presumably small substrates such as fluoride anion, methanol and acetonitrile can fit into the binding cavities easily without requiring substantial changes in conformation. Consistent with this assumption was the observation that significant differences in binding affinity were observed between the individual configurational isomers. For example, the ααββ isomer of **45**, the isomer with most open binding cavity was found to have around four times higher affinity for the bulkier chloride anion, as compared to the corresponding αααβ and αααα isomers (of **45**).

Table 7
Association constants for compounds **45** and **46** (mol^{-1} dm^3) with anionic substrates [a] in acetonitrile-d_3 (0.5% v/v D_2O) at 22°C. Corresponding association constants for *meso*-octamethylcalix[4]pyrrole **1** are also listed for comparison. Data taken from Ref. [28]

	Compound						
	1	**45**			**46**		
Isomer		ααββ	αααβ	αααα	ααββ	αααβ	αααα
Fluoride	>10,000	>10,000	5000 [b]	>10,000 [c]	4600	1100 [b]	>10,000
Chloride	>5000	1400 [d]	260	320	<100	220	300
Phosphate	1300	520 [d]	230	500	<100	<80	<100

[a] Acetonitrile-d_3 (0.5% v/v D_2O) solutions of receptors **1**, **45** and **46** (4.5 and 4.6×10^{-5} mol dm^{-3}, respectively) were titrated by adding concentrated acetonitrile-d_3 (0.5% v/v D_2O) solutions of the anions in question (in the form of their tetrabutylammonium salts) that, to account for dilution effects, also contained **1**, **45** and **46** at their initial concentrations. Estimated errors were <15%. Binding stoichiometries, determined by Job plots, were 1:1 unless otherwise indicated.

[b] Fit by following the change of two different β-pyrrole CH resonances.

[c] At high [F^-]/[calixpyrrole] ratios, a second binding process, involving presumably interactions between the fluoride and the phenolic OH residues, is observed.

[d] Fit by following both the change of *meso*-aryl CH and β-pyrrole CH resonances.

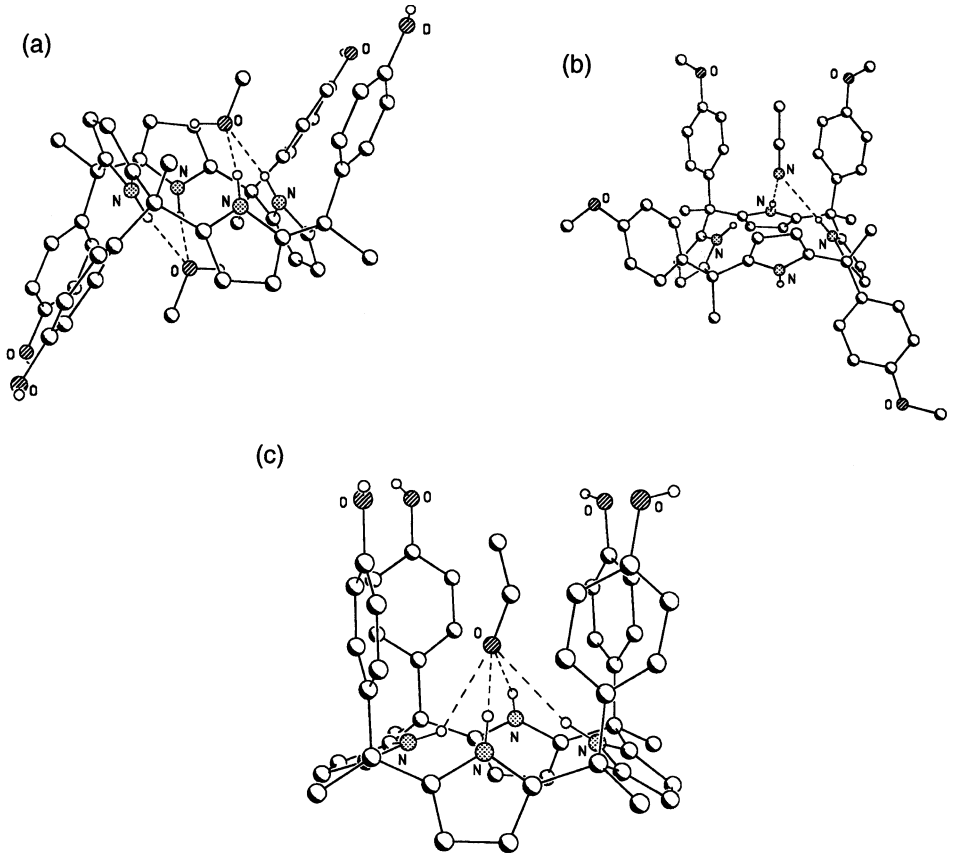

Fig. 17. Side views of: (a) the ααββ isomer of tetra-(4-hydroxyphenyl)calix[4]pyrrole (**45**); (b) the αααβ isomer of tetra-(4-methoxyphenyl)calix[4]pyrrole (**46**), obtained by methylation of the corresponding hydroxyderivative; and (c) the αααα isomer of tetra-(4-hydroxyphenyl)calix[4]pyrrole (**45**). Diagrams produced using data from the Cambridge Crystallographic Database.

It is also important to note that electronic factors proved significant, in spite of the long distance between the *meso*-aryl substituents and pyrrole NH hydrogen bond donor atoms involved in actual anion recognition. For instance, each of the isomers of **45** was found to display a considerably higher affinity for anions than did the corresponding isomers of the methoxy substituted system, **46**. Further, as a general rule the anion affinities of both species were found to be less than those of **1**, an unexpected result that contradicts the, perhaps, intuitively appealing expectation that the deep cavities of **45** and **46** would serve to increase anion affinities in absolute terms.

Another unexpected outcome of our studies and those of the Floriani group was the finding that systems such as **45** and **56** self-assemble in the solid state to form a variety of self-assembled supramolecular architectures. Three such representative arrays, all formed from the αααα isomer of **45** are shown in Fig. 18 [28,30].

By extending the cavity of the αααα-isomer of **45** it has been possible to 'switch-off' the binding of anions other than fluoride in DMSO-d_6 solution [31]. Specifically, two new 'super-extended cavity' calix[4]pyrroles bearing ester (**47**) and amide (**48**) functionalities were prepared using an adaptation of synthetic techniques first developed in the context of calix[4]*arene* chemistry [32]. In DMSO-d_6, these receptors were found not to interact with chloride, bromide, iodide, dihydrogen phosphate or hydrogen sulfate anions. On the other hand, the addition of fluoride anion to solutions of either **47** or **48**, gave rise to new resonances in the ^{1}H-NMR spectrum that are best rationalized in terms of the formation of 1:1 fluoride complexes (Fig. 19). Interestingly, the grow-in of new peaks, rather than displacement (shifting) of existing ones, is consistent with complexation/decomplexation occurring under conditions of slow exchange, behavior not previously observed with calix[4]pyrroles at room temperature. Perhaps as a consequence of this slow exchange, coupling between the bound fluoride anion and the calixpyrrole NH groups was readily observed; it resulted in the NH resonance, normally a singlet, appearing as a doublet with a ^{19}F–^{1}H coupling constant of 47 Hz.

Systems such as **47** and **48**, while still the subject of ongoing study, look especially attractive as precursors for the generation of selective fluoride anion sensors. In particular, because only the fluoride anion is bound by these receptors, with no detectable affinity being observed for other potentially competing species (e.g. chloride anion, dihydrogen phosphate anion) in DMSO-d_6, it should allow this particular anionic analyte to be detected at substoichiometric concentrations in the presence of a large excess of one or more potential interferants.

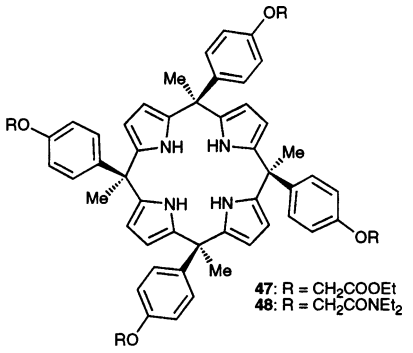

7. *N*-confused calix[4]pyrroles

The synthesis of *N*-confused porphyrins has been the goal of a number of research groups over the last few years [33,34]. Surprisingly, up until recently there were no confirmed examples of *N*-confused calixpyrroles [35]. However, in 1999 Dehaen and co-workers found that by systematically varying the reaction conditions used to produce *meso*-tetraspirocyclohexylcalix[4]pyrrole **49**, it is possible to isolate a variety of *N*-confused calix[4]pyrroles (e.g. **50** and **51**) [36]. In these

studies, equimolar mixtures of pyrrole and cyclohexanone were heated for 4 h at reflux with the choice of solvents and acid catalysts being varied. The results of these trials are shown in Table 8.

The isomers produced by the above studies were identified in part using ^{1}H- and ^{13}C-NMR spectroscopy, with the symmetry of the regular calix[4]pyrrole **49** being completely broken in the singly *N*-confused isomer **50**. The doubly confused isomers **51** proved less soluble than the singly confused isomer **50** and in this case

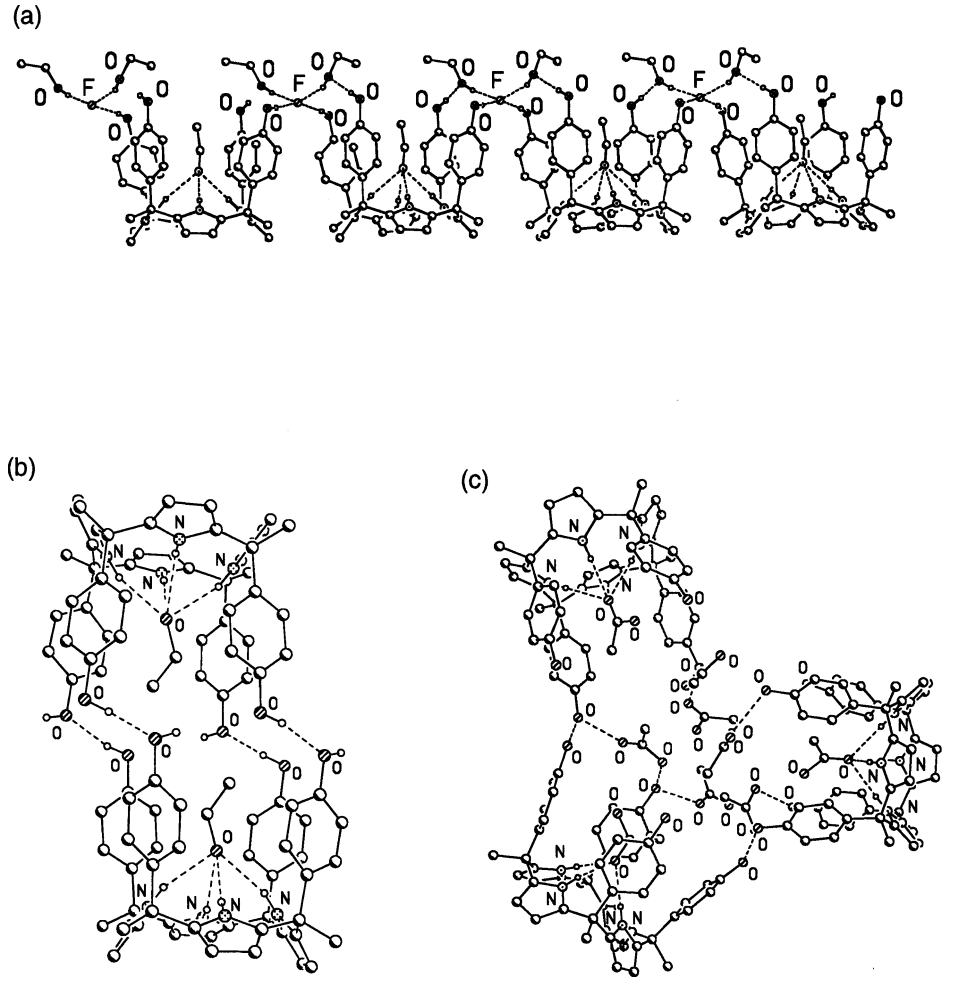

Fig. 18. In the presence of fluoride anion and a hydrogen-bonding competitor, such as ethanol, the αααα isomer of **45** forms an "outside templated" molecular ribbon (a) in the solid state. In the absence of a templating anion, the same compound crystallizes in the form of well-defined "molecular boxes" (b). The very same compound, upon crystallization from acetic acid forms hydrogen bonded cyclic trimers (c). Diagrams produced using data from the Cambridge Crystallographic Database.

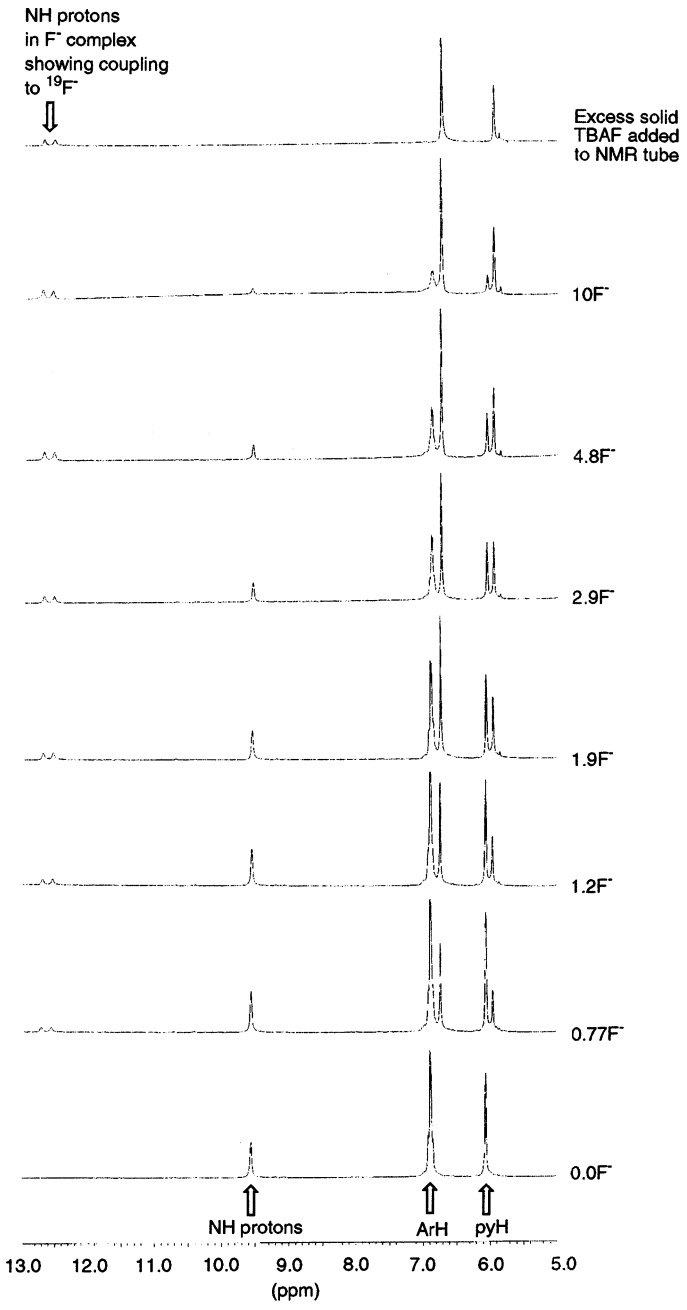

Fig. 19. Changes in the ^{1}H-NMR spectra of compound **48** in deuterated DMSO solution observed upon the addition of aliquots of tetrabutylammonium fluoride. Proton resonances corresponding to the free receptor and fluoride complex can be seen in addition to coupling between the NH proton and the bound $^{19}F^{-}$ nucleus. (Reproduced with permission from Chem. Commun. (2000) 1129, Copyright 2000, The Royal Society of Chemistry.)

Table 8
Results of the condensation of pyrrole and cyclohexanone at reflux (4 h) in a variety of solvents using a number of different acid catalysts. Product **49** is the normal calixpyrrole, **50** the *N*-confused calixpyrrole, and **51** the isomeric mixture of the doubly *N*-confused calix[4]pyrroles. Data taken from Ref. [36]

Entry	Solvent	Catalyst	Total	Yield (%)		
				49	**50**	**51**
A	Ethanol	Conc. HCl	74	62	12	0
B	Ethanol	CH_3SO_3H	87	66	22	0
C	Ethanol	$BF_3{\cdot}Et_2O$	94	73	21	0
D	Ethanol	CF_3COOH	97(87) [a]	80(77) [a]	18(10) [a]	0(0) [a]
E	Ethanol	p-$CH_3C_6H_4SO_3H$	91	69	17	5
F	Ethanol	$ZnCl_2$	44	31	13	0
G	No solvent [b]	CH_3SO_3H	34	12	22	0
H	$CHCl_3$	CF_3COOH	87	80	3	4
I	$CHCl_3$	p-$CH_3C_6H_4SO_3H$	90(70) [a]	53(9) [a]	5(4) [a]	32(57) [a]
J	Benzene	p-$CH_3C_6H_4SO_3H$	94	54	6	35
K	Toluene	p-$CH_3C_6H_4SO_3H$	64	18	11	36
L	Toluene	CF_3COOH	90	77	16	1
M	Petroleum ether	CH_3SO_3H	53	42	11	0
N	Ethanol	CF_3COOH	9 [c]	65 [c]	26 [c]	0

[a] Yields in parentheses refer to heating at reflux of 60 h.
[b] No solvent was used. Stirring became difficult because of the immediate formation of the calixpyrrole and the reaction was worked up at this point.
[c] Condensation of acetone and pyrrole.

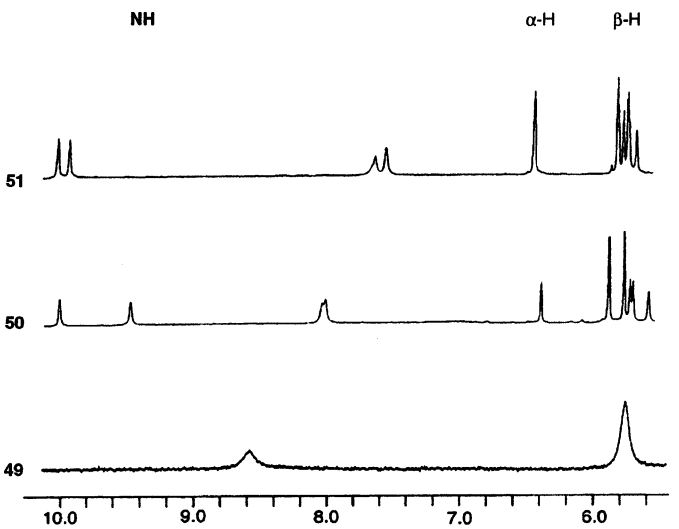

Fig. 20. The pyrrole region of the ^{1}H-NMR spectra of **49**, **50**, and **51** (as a mixture of isomers **51a**–**e**). (Reproduced with permission from Angew. Chem. Int. Ed. Engl. 38 (1999) 3359, Copyright 1998, Wiley–VCH.)

it was not possible to obtain a full ^{13}C-NMR spectrum. The proton NMR spectra of **49**, **50**, and the isomeric mixture **51** are shown in Fig. 20.

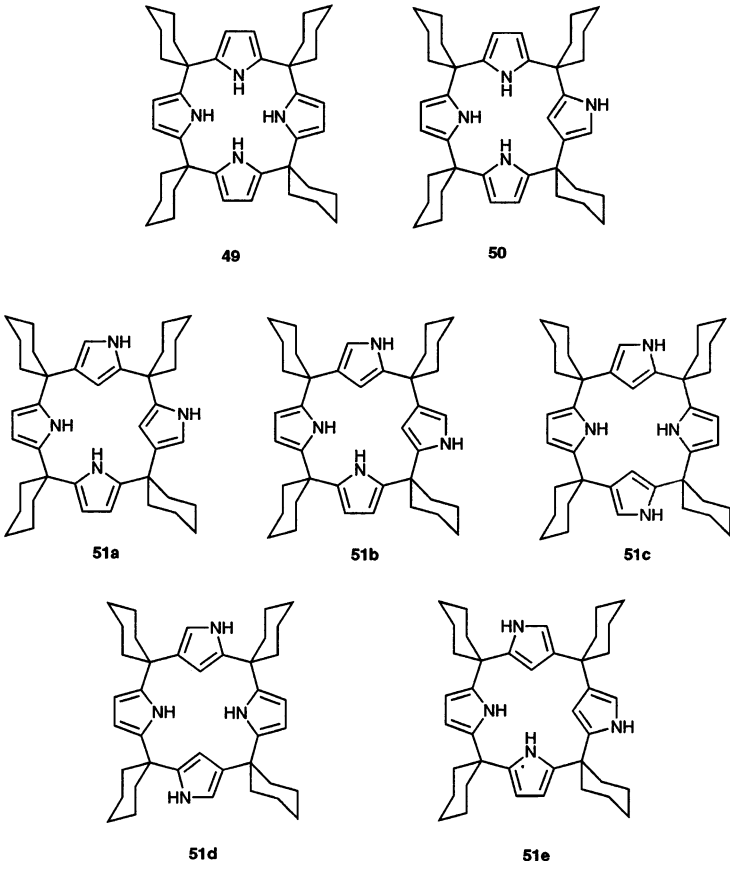

8. Higher order calix[4]pyrroles

Inspired by the basic, predicative analogy we have put forward to relate the chemistry of calixpyrroles to that of the calixarenes, we realized that "expanded" or so-called "higher order" calix[*n*]pyrroles ($n > 4$) might display anion binding properties very different from their tetrameric counterparts, in particular displaying selectivity for larger anions. Unfortunately, at the start of our studies a clean sample of a higher order calixpyrrole had yet to be prepared. While initial analyses of the reaction mixtures used to produce *meso*-octamethylcalix[4]pyrrole **1** did reveal traces of higher order macrocycles, all efforts to isolate the putative calix[*n*]pyrrole ($n > 4$) products proved unsuccessful [2]. Thus, we elected to pursue a template-based strategy [29,37]. Specifically, by using *p-tert*-butylcalix[5]arene pentaketone **52**, a material prepared by Prof. Tony McKervey and his group at Queen's University, Belfast, as both a reactant and template, it proved possible to

prepare the calix[5]arene–calix[5]pyrrole pseudo-dimer **53** in 10% yield from pyrrole in the presence of $BF_3{\cdot}Et_2O$ as a catalyst (Scheme 11). Unfortunately, because of the nature of the template strategy employed, it proved impossible to prepare free calix[5]pyrrole from **53**. Further, compound **53** itself was found to display little, if any, affinity for anions. This latter result, although disappointing, was not considered surprising in light of the fact that the pyrrolic NH groups were found to be "tied up" in intramolecular hydrogen bonds with the phenolic oxygen atoms at the lower rim of the calix[5]arene.

The first synthesis of a well-characterized higher order calixpyrrole, specifically calix[6]pyrrole, was achieved by Eichen and co-workers in 1998 [38]. These researchers used a step-wise procedure that involved condensing pyrrole with sterically bulky diketones, such as benzophenone, di-(2-pyridyl)ketone, and 9-fluorenone, to produce di-(2-pyrrolyl)methanes (**54**, **55** and **56**: Scheme 12). These intermediate products failed to react further with the corresponding ketone (to produce, e.g. the expected calix[4]pyrrole). However, it was found that they could be condensed with acetone in the presence of $BF_3{\cdot}OEt_2$ to produce calix[4]pyrroles with different substituents in the *meso*-positions (**57**, **58** and **59**). Further, and more significantly, in the presence of trifluoroacetic acid this second step was found to proceed along a different course, producing the calix[6]pyrroles **60** and **61** in isolated yields of 25 and 2%, respectively. X-ray crystallographic analysis of the calix[6]pyrrole **60** revealed that the macrocycles adopt an asymmetric cone-like conformation in which all three diphenylmethylene bridges point above the macrocyclic plane (Fig. 21).

In a separate, but highly complementary, work Kohnke and co-workers found that *meso*-dodecamethylcalix[6]pyrrole **68**, as well as *meso*-dodecamethylcalix[3]furan[3]pyrrole **66** and *meso*-dodecamethylcalix[2]furan[4]pyrrole **67** may be prepared from *meso*-dodecamethylcalix[6]furan **62** (Scheme 13) [39]. Specifically, these investigators discovered that reaction of the calix[6]furan **62** with *m*-CPBA followed by zinc/AcOH serves to open some or all of the furan heterocycles in the ring; this produces a set of ring-contained α,β-diketones that may be converted to pyrrole by reaction with ammonium acetate (Scheme 13). The crystal structure of the *meso*-dodecamethylcalix[6]pyrrole macrocycle **68** is shown in Fig. 22a, whereas that of the corresponding [3]furan[3]pyrrole system, **66**, is shown in Fig. 22b.

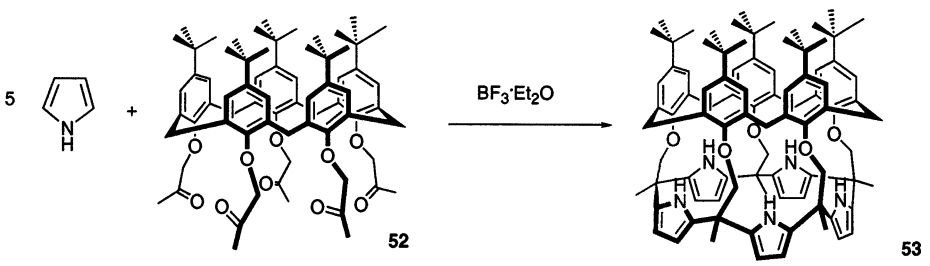

Scheme 11.

Transport studies were carried out in an effort to compare the ability of *meso*-octamethylcalix[4]pyrrole and *meso*-dodecamethylcalix[6]pyrrole to transport halide anions from an aqueous (D_2O) to an organic (CD_2Cl_2) phase [40]. The results of these studies are shown in Table 9. They indicate that *meso*-dodecamethylcalix[6]pyrrole **68** is capable of extracting bromide and chloride anions from D_2O to CD_2Cl_2, with a more efficient extraction being observed for chloride.

Single crystal X-ray diffraction quality crystals of both the chloride and bromide complexes of *meso*-dodecamethylcalix[6]pyrrole **68** were obtained and elucidation of the crystal structures revealed that the anions are coordinated at the center of the macrocycle via six NH–Cl/Br hydrogen bonds (Fig. 22c and d). The N···Cl and H···Cl distances range from 3.265(7) to 3.305(7) Å and 2.39 to 2.42 Å, respectively, while the N···Br and H···Br distances range from 3.344(5) to 3.404(5) Å and 2.46 to 2.51 Å, respectively. Taken in conjunction with the transport studies, these findings provide support for the contention that calix[6]pyrroles (and other higher order calix[*n*]pyrroles) could show selectivity for larger anions. As yet, however, no actual

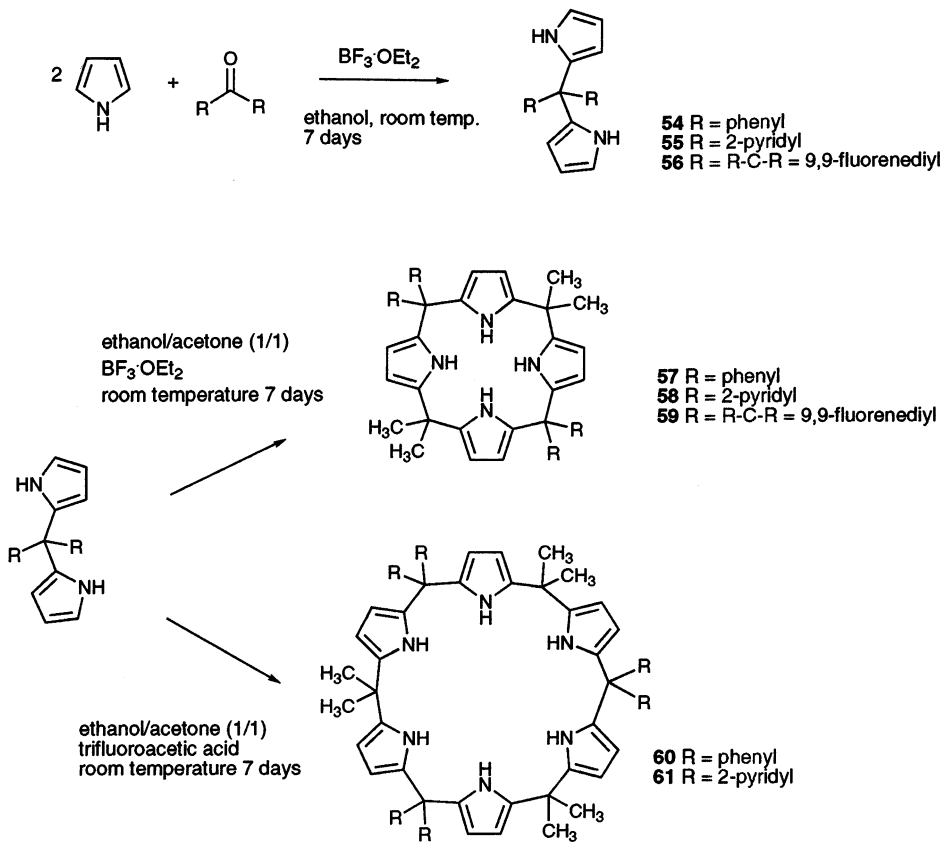

Scheme 12.

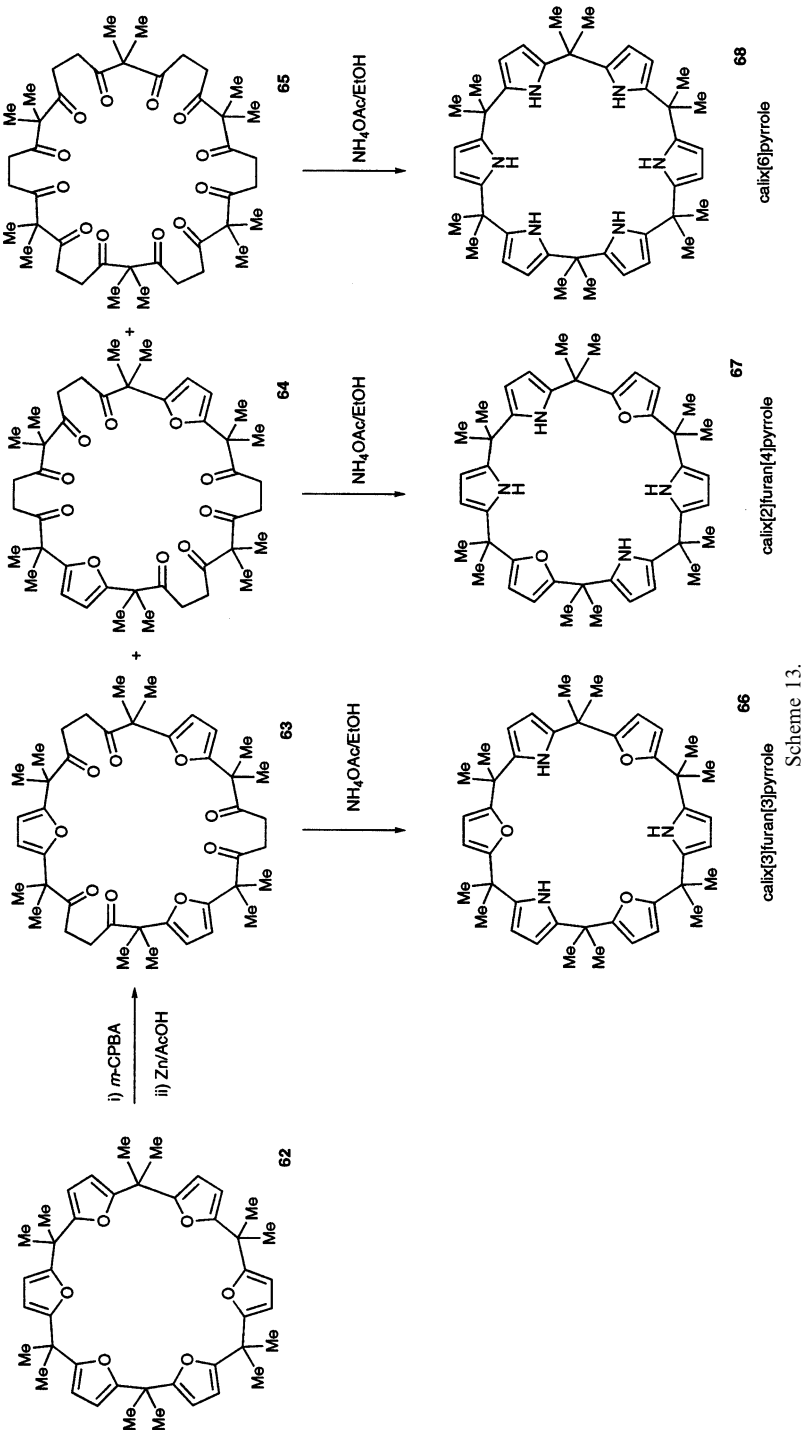
62
i) m-CPBA
ii) Zn/AcOH
63
64
65
NH4OAc/EtOH
NH4OAc/EtOH
NH4OAc/EtOH
66
calix[3]furan[3]pyrrole
67
calix[2]furan[4]pyrrole
68
calix[6]pyrrole

Scheme 13.

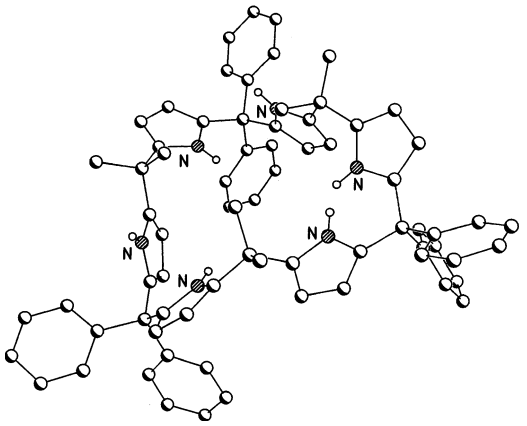

Fig. 21. The crystal structure of calix[6]pyrrole **60**. Diagram produced using data from the Cambridge Crystallographic Database.

anion–calix[6]pyrrole association constants have been reported by either Kohnke or Eichen.

In a work that provides an important complement to that of Kohnke, Lee and co-workers succeeded in synthesizing a variety of calix[*m*]thieno[*n*]pyrrole and calix[*m*]furano[*n*]pyrrole macrocycles using a stepwise strategy [41,42]. For instance, these researchers found that reaction of furan or thiophene with butyl lithium and acetone affords a 2,5-diol that reacts with pyrrole in the presence of BF_3 to afford the oxa- or thia-tripyrromethane **73** or **74**. Subsequent reaction of **73** or **74** with **71** or **72** (Scheme 14) affords a variety of mixed calixfuranothienopyrrole macrocycles with ring sizes ranging from four (**75**, **76**, **81**) through six (**77**, **78**, **82**) to eight (**79**, **80**, **83**) heterocycles [41]. To date, the molecular recognition properties of these compounds have not been reported. Nor, have confirming X-ray structural analyses been put forward for many of the new systems produced. On the other hand, the work of Lee does represent an important new line of research in the macrocyclic area that is made further attractive by the possibility that it could lead to the construction of "extra large" calix[*n*]pyrroles via the application of Kohnke procedure.

Most recently, a direct synthesis of higher order calixpyrroles has been discovered. It came about as the result of a thorough re-examination of the acid-catalyzed pyrrole–acetone condensation reaction. In the process of this re-examination, we discovered that the use of 3,4-difluoropyrrole, rather than simple pyrrole, allows for the preparation of calix[5]- and calix[8]pyrroles [43]. Apparently, as the result of using the less reactive 3,4-difluoropyrrole in the condensation, the macrocylization reaction proceeds under kinetic, rather than thermodynamic, control at ambient temperature. For presumably related electronic reasons, the condensation products are also stable and, in favorable cases, may be isolated via chromatographic means. Depending on the exact ratio and concentration of fluorinated pyrrole and acetone employed (MeOH solvent, methane sulfonic acid catalyst), three products, namely

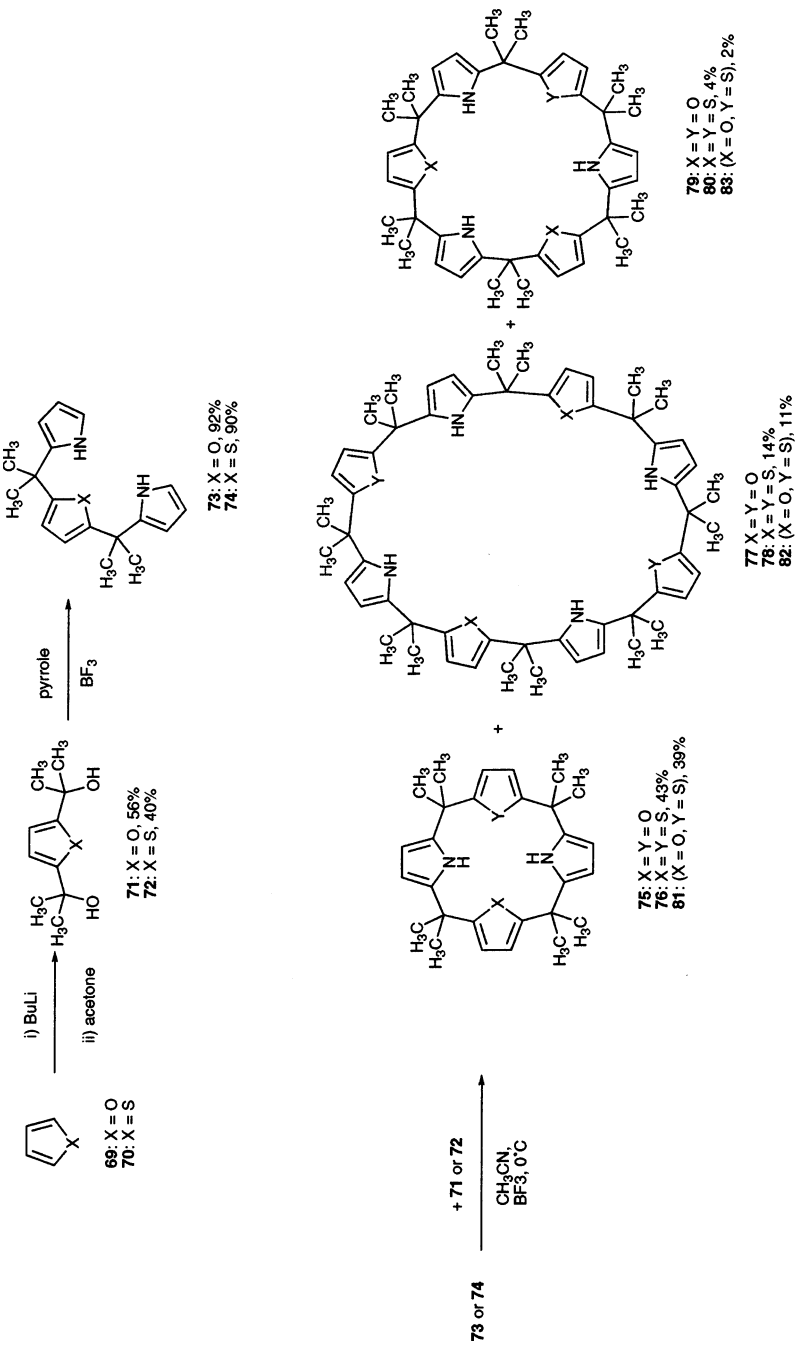
69: X = O
70: X = S
i) BuLi
ii) acetone
71: X = O, 56%
72: X = S, 40%
pyrrole
BF3
73: X = O, 92%
74: X = S, 90%
73 or 74
+ 71 or 72
CH3CN, BF3, 0°C
75: X = Y = O
76: X = Y = S, 43%
81: (X = O, Y = S), 39%
77 X = Y = O
78: X = Y = S, 14%
82: (X = O, Y = S), 11%
79: X = Y = O
80: X = Y = S, 4%
83: (X = O, Y = S), 2%

Scheme 14.

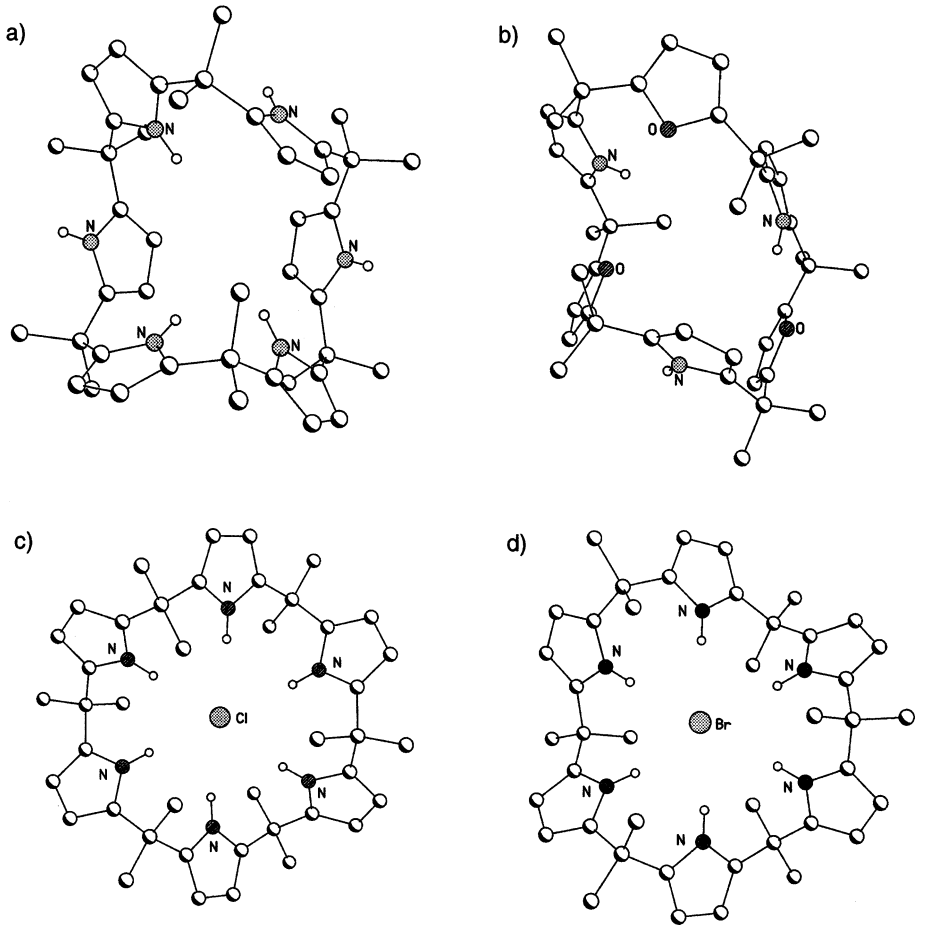

Fig. 22. The crystal structures of: (a) *meso*-dodecamethylcalix[6]pyrrole **68**; (b) *meso*-dodecamethylcalix[3]furan[3]pyrrole **66**; (c) chloride; and (d) bromide complexes of calix[6]pyrrole **68**. Diagrams produced using data from the Cambridge Crystallographic Database.

the calix[4]pyrrole **84**, calix[5]pyrrole **85**, and calix[8]pyrrole **86**, may be isolated in yields of up to 85, 23, and 14%, respectively (Scheme 15). To the best of our knowledge, the octapyrrolic system **86** represents the largest pure calix[*n*]pyrrole characterized to date.

Fig. 23 provides a view of four different crystal structures of the cyclic tetramer **84**. These structures are of interest because they represent the first ''matched set'', wherein the same calix[4]pyrrole has been characterized structurally in each of the four possible conformations. By contrast, the crystal structures of the *meso*-decamethyl-decafluorocalix[5]pyrrole **85** and *meso*-hexadecamethyl-hexadecafluorocalix[8]pyrrole **86**, shown in Fig. 24, are of interest because they provide unequivocal proof that these higher order calixpyrroles can indeed be made and,

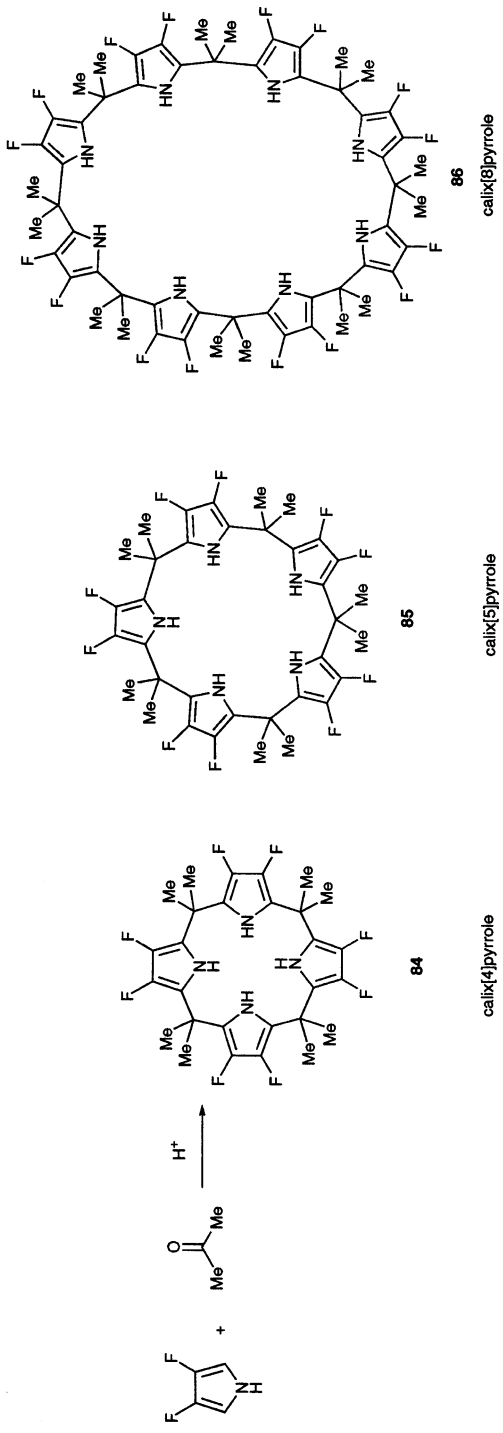

Scheme 15.

Table 9
Transfer of tetrabutylammonium halide salts between D_2O and CD_2Cl_2 at 16°C with and without *meso*-octamethylcalix[4]pyrrole and *meso*-dodecamethylcalix[6]pyrrole. The figures indicate percentage variation in the concentration of the salt in each phase after equilibration and were reproducible within a $\pm 2\%$ error. Data taken from Ref. [40]

	Macrocycle					
	None		*meso*-Octamethylcalix[4]pyrrole **1**		*meso*-Dodecamethylcalix[6] pyrrole **68**	
	D_2O	CD_2Cl_2	D_2O	CD_2Cl_2	D_2O	CD_2Cl_2
n-Bu_4NF	[a]	[b]	[a]	[a]	[a]	[a]
n-Bu_4NCl	−4	[b]	−4	+4	−65	+65
n-Bu_4NBr	−20	[b]	−22	+22	−31	+31
n-Bu_4NI	−86	[b]	−86	+86	−86	+86

[a] Value within experimental error (<2%).
[b] The percentage variation was not measured.

once made, can adopt conformations wherein NH rich central hydrogen bond donor cavities exist.

The successful preparation of polyfluorinated calixpyrroles is a particularly significant result in the light of the previous findings that calix[4]pyrroles with electron withdrawing substituents on the β-pyrrolic positions show augmented affinity for anions [9]. In fact, relative to **1**, the octafluorocalix[4]pyrrole **84** was found to show not only enhanced affinities for various anionic substrates but also improved selectivities for phosphate and chloride anions (Table 10) [44].

At present, work with **85** and **86** is still in its early stages. Thus, the question of whether these calix[5]- and calix[8]pyrrole systems display anion selectivities that are altered or improved remains unanswered. Still, in preliminary work, it has been found that the decafluorocalix[5]pyrrole **85** exhibits an affinity for chloride anion ($K_a = 41{,}000\ mol^{-1}\ dm^3$) that is increased by a factor of roughly four relative to the corresponding octafluorocalix[4]pyrrole congener **84** ($K_a = 11{,}000\ mol^{-1}\ dm^3$) as observed by both ^1H- and ^{19}F-NMR titration experiments in acetonitrile-d_3 (0.5% D_2O).

9. Conclusions

The chemistry of calixpyrroles has blossomed considerably over the last three years. Particularly important developments have been seen in the use of calix[4]pyrroles as anion sensors in both the optical and electrochemical realms. It is likely that this work will continue apace abetted by the increased availability of modified, functionalized, and deep cavity calix[4]pyrroles that are expected to show ever-increasing affinities and selectivities. The promise of improved selectivities and

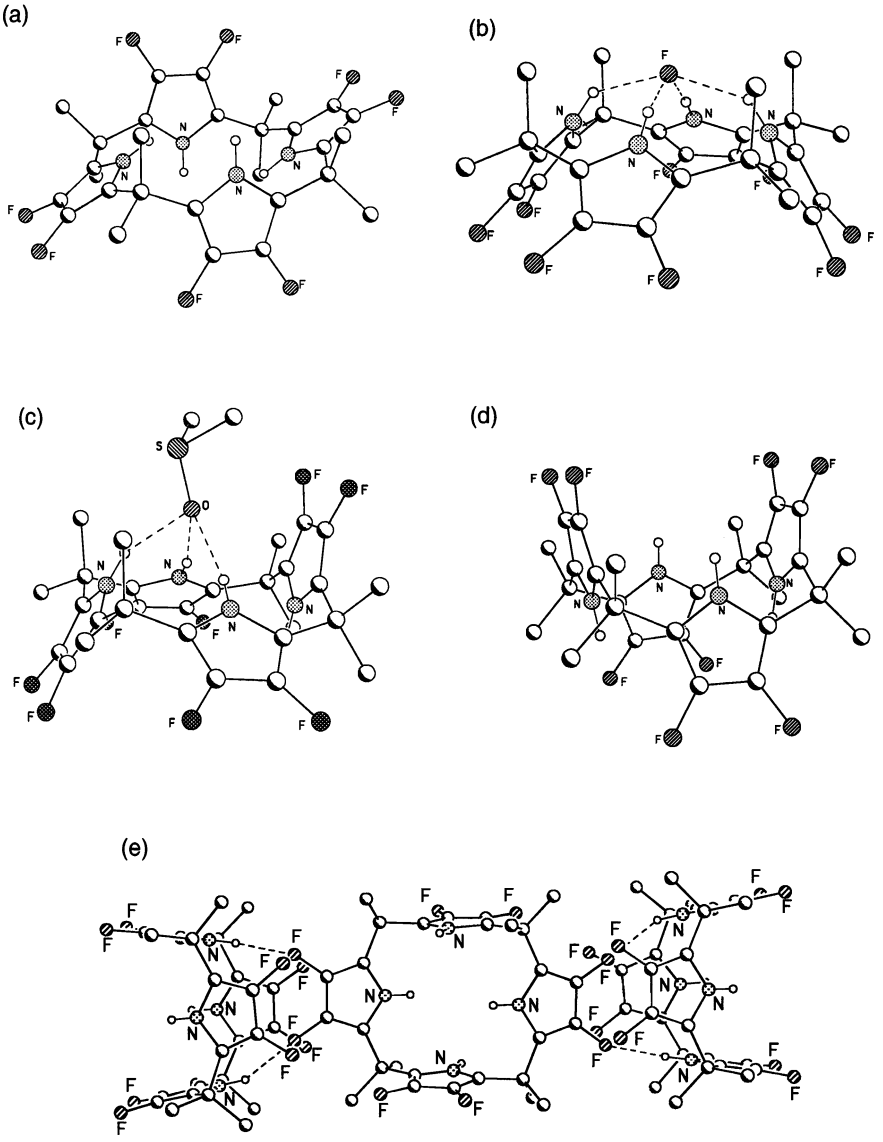

Fig. 23. The crystal structures of receptor **84** adopting the: (a) 1,2-alternate conformation (crystallized from MeOH–CH_2Cl_2); (b) the cone conformation in the fluoride complex; (c) the partial cone conformation (crystallized from DMSO); and (d) the 1,3-alternate conformation (crystallized from MeOH–CH_2Cl_2). The 1,2- and 1,3-conformers are observed in the same crystal with the packing diagram shown in (e) revealing β–F···HN hydrogen bonds. Diagrams produced using data from the Cambridge Crystallographic Database.

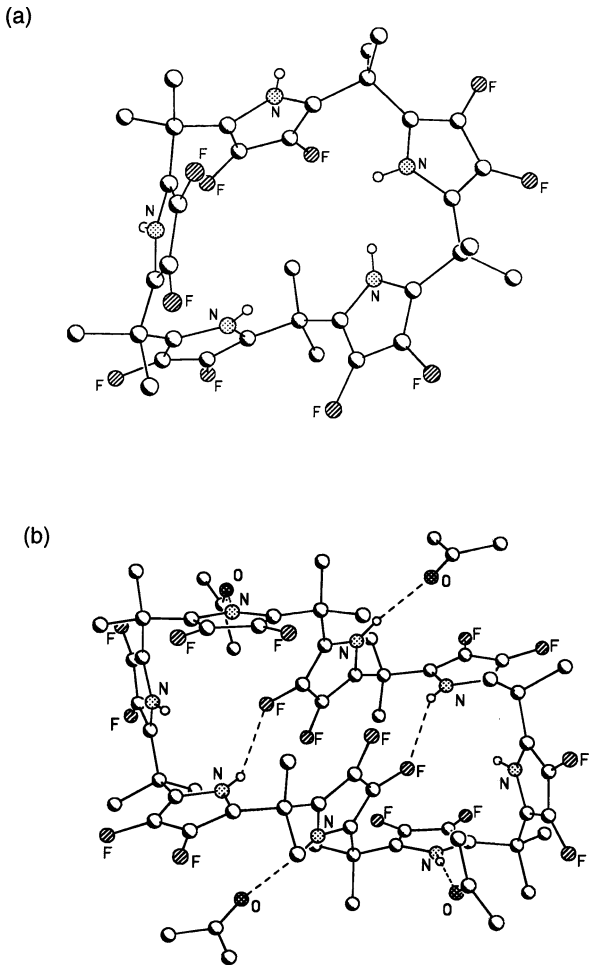

Fig. 24. The crystal structures of *meso*-dodecamethyldecafluorocalix[5]pyrrole **85**, *meso*-hexadecamethylhexadecafluorocalix[8]pyrrole **86**. Diagrams produced using data provided by Dr Vincent Lynch of the Department of Chemistry and Biochemistry, The University of Texas at Austin.

augmented affinities is also likely to be met through the continued development of higher order calixpyrroles. Here, the discovery recently of three separate, but fully viable, synthetic strategies is likely to prove seminal; it leads to the conclusion that calixpyrroles will continue to grow, not only in size, but also in importance, in the years to come.

Table 10
Association constants for **1** and **84** ($mol^{-1}\,dm^3$) for anionic substrates [a] and DMSO-d_6 as a neutral substrate recorded in acetonitrile-d_3 (0.5% v/v D_2O) at 22°C. Data taken from Ref. [44]

Anion	Compound **1**	Compound **84** [b]	$R_{84/1}$ [c]
F^-	>10,000	17,100	≥1.71
Cl^-	5000	10,700	2.14
$H_2PO_4^-$	1300	9100	7.0
DMSO-d_6	<5 [d]	20	>4.0

[a] The anions used in this study were in the form of their tetrabutylammonium salts.
[b] The solutions contain both monomeric and aggregated species. Fits were performed for the monomeric fraction of **84** using both pyrrole NH and pyrrole F resonances in the ^{1}H-NMR and ^{19}F-NMR spectra, respectively. For **84** the calculated affinity constants were found to be independent of concentration over the concentration range of 4 mM ≤ [**84**] ≤ 14 mM. All errors were ≤20%.
[c] Refers to the ratio of association constants recorded for **84** and **1**.
[d] The interaction of **1** with DMSO-d_6 is too weak to allow for a more accurate estimation of the relevant association constant.

Acknowledgements

We would like to thank Dr Vince Lynch (The University of Texas at Austin) and Dr Simon J. Coles (University of Southampton) for help with the preparation of the crystallographic figures in this review. This work was supported by the National Science Foundation (grant no. CHE 9725399 to J.L.S.), the National Institutes of Health (grant no. GM 58907 to J.L.S.), the Texas Advanced Research (grant ARP-102 to J.L.S.) program, the Royal Society (University Research Fellowship to P.A.G.) and the EPSRC (fast stream studentship grant to P.A.G.)

References

[1] A. Baeyer, Ber. Dtsch. Chem. Ges. 19 (1886) 2184.
[2] (a) P.A. Gale, J.L. Sessler, V. Král, V. Lynch, J. Am. Chem. Soc. 118 (1996) 5140. (b) J.L. Sessler P.A. Gale, The Porphyrin Handbook, in: K.M. Kadish, K.M. Smith, R. Guilard (Eds.), vol. 6, Academic Press, San Diego, CA, 2000, pp. 257–278.
[3] W.E. Allen, P.A. Gale, C.T. Brown, V.M. Lynch, J.L. Sessler, J. Am. Chem. Soc. 118 (1996) 12,471.
[4] C.D. Gutsche, Calixarenes revisited, in: J.F. Stoddart (Ed.), Monographs in Supramolecular Chemistry, Royal Society of Chemistry, Cambridge, 1998.
[5] P.A. Gale, J.L. Sessler, V. Kral, Chem. Commun. (1998) 1.
[6] C. Floriani, R. Floriani-Moro, K.M. Kadish, K.M. Smith, R. Guilard (Eds.), The Porphyrin Handbook, vol. 3, Academic Press, San Diego, CA, 2000, pp. 405–420.
[7] C. Floriani, R. Floriani-Moro, in: K.M. Kadish, K.M. Smith, R. Guilard (Eds.), The Porphyrin Handbook, vol. 3, Academic Press, San Diego, CA, 2000, pp. 385–403.
[8] V. Král, J.L. Sessler, R.S. Zimmerman, D. Seidel, V. Lynch, B. Andrioletti, Angew. Chem. Int. Ed. Engl. 39 (2000) 1055.
[9] (a) P.A. Gale, J.L. Sessler, W.E. Allen, N.A. Tvermoes, V. Lynch, Chem. Commun. (1997) 665. (b) J.L. Sessler, P. Anzenbacher Jr, H. Miyaji, K. Jursíková, E.R. Bleasdale P.A. Gale, Ind. Engng Chem. Res. 39 (2000) 3471.

[10] P. Anzenbacher Jr, K. Jursíková, J.A. Shriver, H. Miyaji, V.M. Lynch, J.L. Sessler, P.A. Gale, J. Org. Chem. 65 (2001) 7641.
[11] H. Miyaji, W. Sato, J.L. Sessler, V.M. Lynch, Tetrahedron Lett. 41 (2000) 1369.
[12] W. Sato, H. Miyaji, J.L. Sessler, Tetrahedron Lett. 41 (2000) 6731.
[13] Y. Furusho, H. Kawasaki, S. Nakanishi, T. Aida, T. Takata, Tetrahedron Lett. 39 (1998) 3537.
[14] C. Floriani, Chem. Commun. (1996) 1257.
[15] J.L. Sessler, A. Andrievsky, P.A. Gale, V. Lynch, Angew. Chem. Int. Ed. Engl. 35 (1996) 2782.
[16] P. Anzenbacher Jr, K. Jursíková, J.L. Sessler, J. Am. Chem. Soc. 122 (2000) 9340.
[17] W.P. van Hoorn, W.L. Jorgensen, J. Org. Chem. 64 (1999) 7439.
[18] A. Metzger, E.V. Anslyn, Angew. Chem. Int. Ed. Engl. 37 (1998) 649.
[19] P.A. Gale, L.J. Twyman, C.I. Handlin, J.L. Sessler, Chem. Commun. (1999) 1851.
[20] H. Miyaji, P. Anzenbacher Jr., J.L. Sessler, E.R. Bleasdale, P.A. Gale, Chem. Commun. (1999) 1723.
[21] H. Miyaji, W. Sato, J.L. Sessler, Angew. Chem. Int. Ed. Engl. 39 (2000) 1777.
[22] V. Král, J.L. Sessler, T.V. Shishkanova, P.A. Gale, R. Volf, J. Am. Chem. Soc. 121 (1999) 8771.
[23] V. Král, P.A. Gale, P. Anzenbacher Jr., K. Jursíková, V. Lynch, J.L. Sessler, Chem. Commun. (1998) 9.
[24] P.D. Beer, P.A. Gale, Z. Chen, J. Chem. Soc. Dalton Trans. (1999) 1897.
[25] J.L. Sessler, A. Gebauer, P.A. Gale, Gazz. Chim. Ital. 127 (1997) 723.
[26] Z. Chen, P.A. Gale, P.D. Beer, J. Electroanal. Chem. 393 (1995) 113.
[27] P.A. Gale, E.R. Bleasdale, G.Z. Chen, Supramol. Chem. (2001), in press.
[28] P. Anzenbacher Jr., K. Jursiková, V.M. Lynch, P.A. Gale, J.L. Sessler, J. Am. Chem. Soc. 121 (1999) 11,020.
[29] P.A. Gale, J.W. Genge, V. Král, M.A. McKervey, J.L. Sessler, A. Walker, Tetrahedron Lett. 38 (1997) 8444.
[30] L. Bonomo, E. Solari, G. Toraman, R. Scopelliti, M. Latronico, C. Floriani, Chem. Commun. (1999) 2413.
[31] S. Camiolo P.A. Gale, Chem. Commun. (2000) 1129.
[32] F. Arnaud-Neu, E.M. Collins, M. Deasy, G. Ferguson, S.J. Harris, B. Kaitner, A.J. Lough, M.A. McKervey, E. Marques, B.L. Ruhl, M.J. Schwing-Weill, E.M. Seward, J. Am. Chem. Soc. 111 (1989) 8681.
[33] L. Latos-Grazynski, P.J. Chimielewski, New. J. Chem. 27 (1997) 691.
[34] K. Ariga, T. Kunitake, H. Furuta, J. Chem. Soc. Perkin Trans. 2 (1996) 667.
[35] O. Tsuge, M. Tashiro, Y. Kiryu, Org. Prep. Proc. Int. 7 (1975) 39.
[36] S. Depraetere, M. Smet, W. Dehaen, Angew. Chem. Int. Ed. Engl. 38 (1999) 3359.
[37] P.A. Gale, J.L. Sessler, V. Lynch, P.I. Sansom, Tetrahedron Lett. 37 (1996) 7881.
[38] B. Turner, M. Botoshansky, Y. Eichen, Angew. Chem. Int. Ed. Engl. 37 (1998) 2475.
[39] G. Cafeo, F.H. Kohnke, G.L.L. Torre, A.J.P. White, D.J. Williams, Angew. Chem. Int. Ed. Engl. 39 (2000) 1496.
[40] G. Cafeo, F.H. Kohnke, G.L.L. Torre, A.J.P. White, D.J. Williams, Chem. Commun. (2000) 1207.
[41] Y.-S. Jang, H.-J. Kim, P.-H. Lee, C.-H. Lee, Tetrahedron Lett. 41 (2000) 2919.
[42] N. Arumugam, Y. Jang, C.H. Lee, Org. Lett. 2 (2000) 3115.
[43] J.L. Sessler, P. Anzenbacher Jr, J.A. Shriver, K. Jursíková, V.M. Lynch, M. Marquez, J. Am. Chem. Soc. 122 (2000) 12,061.
[44] P. Anzenbacher Jr., A.C. Try, H. Miyaji, K. Jursíková, V.M. Lynch, M. Marquez, J.L. Sessler, J. Am. Chem. Soc. 122 (2000) 10,268.